THE JOURNAL OF BIOLOGICAL CHEMISTRY VOL. 290, NO. 8, pp. 4573–4589, February 20, 2015

Tricyclic Covalent Inhibitors Selectively Target Jak3 through an Active Site Thiol*[S]

Received for publication, July 21, 2014, and in revised form, December 17, 2014 Published, JBC Papers in Press, December 31, 2014, DOI 10.1074/jbc.M114.595181

Eric R. Goedken[1], Maria A. Argiriadi, David L. Banach, Bryan A. Fiamengo, Sage E. Foley, Kristine E. Frank, Jonathan S. George, Christopher M. Harris, Adrian D. Hobson, David C. Ihle, Douglas Marcotte, Philip J. Merta, Mark E. Michalak, Sara E. Murdock, Medha J. Tomlinson, and Jeffrey W. Voss

From the AbbVie Bioresearch Center, Worcester, Massachusetts 01605

Background: Janus kinase 3 (Jak3) inhibitors hold promise for treatment of autoimmunity, but developing selective inhibitors is challenging.

Results: We designed Jak3 inhibitors that avoid inhibition of the other JAKs.

Conclusion: Our inhibitors possess high selectivity against other kinases and can potently inhibit Jak3 activity in cell-based assays.

Significance: This class of irreversible inhibitors may be useful as selective agents of Jak3 inhibition.

The action of Janus kinases (JAKs) is required for multiple cytokine signaling pathways, and as such, JAK inhibitors hold promise for treatment of autoimmune disorders, including rheumatoid arthritis, inflammatory bowel disease, and psoriasis. However, due to high similarity in the active sites of the four members (Jak1, Jak2, Jak3, and Tyk2), developing selective inhibitors within this family is challenging. We have designed and characterized substituted, tricyclic Jak3 inhibitors that selectively avoid inhibition of the other JAKs. This is accomplished through a covalent interaction between an inhibitor containing a terminal electrophile and an active site cysteine (Cys-909). We found that these ATP competitive compounds are irreversible inhibitors of Jak3 enzyme activity *in vitro*. They possess high selectivity against other kinases and can potently (IC_{50} < 100 nM) inhibit Jak3 activity in cell-based assays. These results suggest irreversible inhibitors of this class may be useful selective agents, both as tools to probe Jak3 biology and potentially as therapies for autoimmune diseases.

Due to their widespread role in cytokine signaling, the action of Janus kinases (JAKs) is central to regulating the immune system (1–3). These non-receptor tyrosine kinases serve as critical intracellular enzymatic activators for diverse and important cytokines and signaling hormones, including IL-2, IL-4, IL-6, IL-7, IL-12, IL-13, IFN-γ, IFN-α, EPO, and GM-CSF (4, 5). In these pathways, the tyrosine kinase activity of JAKs is required to phosphorylate receptor chains in order to recruit and ultimately phosphorylate signal transducers and activators of transcription (STAT) molecules (2, 6).

The broad strokes of JAK-STAT signaling have been known for some time, and potential therapeutic intervention using JAK small molecule inhibitors has been suggested since those early experiments (7–10). However, only recently have JAK inhibitors been described with sufficient selectivity against other protein kinases and adequate druglike properties to enable clinical trials (11–13). Although initial studies with JAK inhibitors were aimed at preventing solid organ transplant rejection (13, 14), Pfizer, Incyte, Galapagos, Vertex, and AbbVie have advanced Jak inhibitors to clinical trials for chronic autoimmune diseases, such as rheumatoid arthritis (15). In 2012, Pfizer's tofacitinib (CP-690,550; a Jak1/Jak2/Jak3 inhibitor) was granted Food and Drug Administration approval to treat rheumatoid arthritis (16, 17). However, the long term consequences of inhibiting multiple JAKs are not completely understood (18, 19); nor is the relative contribution of specific JAK isoforms to the overall efficacy seen with pan-JAK inhibitors understood.

Given the diverse roles for JAKs in the immune system and in hematopoiesis, a remaining challenge lies in creating drug molecules with specificity within the JAK family. The four JAKs (Jak1, Jak2, Jak3, and Tyk2) have very similar domain structures. These enzymes contain FERM, Src homology 2, pseudokinase, and catalytic tyrosine kinase domains from their N to C termini, respectively. Moreover, despite only 50–60% identity over the entire kinase domain, the JAKs share very high sequence identity in their enzyme active sites. For example, Jak3 shares ~84% of the residues in its active site with Jak1, ~87% with Jak2, and ~80% with Tyk2. This high conservation makes targeting a specific JAK with traditional ATP-competitive inhibitors difficult (Fig. 1). Indeed, numerous pan-JAK inhibitor compounds have been described (12,

---

* Use of the Industrial Macromolecular Crystallography Association-Collaborative Access Team beamline 17-ID (or 17-BM) at the Advanced Photon Source was supported by the companies of the Industrial Macromolecular Crystallography Association through a contract with Hauptman-Woodward Medical Research Institute. Use of the Advanced Photon Source was supported by the United States Department of Energy, Office of Science, Office of Basic Energy Sciences, under Contract DE-AC02-06CH11357. The authors are/were employees of AbbVie (or Abbott Laboratories prior to separation) and may own AbbVie/Abbott stocks or stock options. Financial support for this work was provided by AbbVie, who participated in the interpretation of data, review, and approval of the manuscript.

[S] This article contains supplemental Methods.

The atomic coordinates and structure factors (code 4QPS) have been deposited in the Protein Data Bank (http://wwpdb.org/).

[1] To whom correspondence should be addressed: AbbVie Bioresearch Center, 100 Research Dr., Worcester, MA 01605. Tel.: 508-688-3511; Fax: 508-754-6742; E-mail: eric.goedken@abbvie.com.

20–24), and structural analyses of inhibitors in Jak1, Jak2, and Tyk2 highlight the difficulty in obtaining strong selectivity within the family (25–28). In addition to potential drug molecules, inhibitors targeting specific members of the JAK family could be useful as chemical biology tools to understand the molecular and physiological function of particular JAKs.

In this report, we present biochemical and cellular analyses of several novel tricycle-based inhibitors that are highly selective for Jak3 and compare them with several previously reported JAK inhibitors (Fig. 2). One of the few differences in the JAK active sites is a unique cysteine residue in Jak3 (Cys-909 in the human sequence). We exploited this difference by targeting Cys-909 with covalent inhibitors. Only 10 other protein kinases, including EGFR and BTK, carry a thiol at this position in the ATP-binding site and can be inhibited by a similar mechanism (Fig. 1) (29–31). Through enzyme analysis and mass spectrometry, we show that such covalent inhibitors irreversibly bind Jak3, leading to exquisite kinome selectivity. Furthermore, these compounds can specifically modulate responses driven by Jak3, but not Jak1 or Jak2, in cell-based assays. As such, we demonstrate that this mechanism of inhibition can lead to Jak3-selective tools, a profile that has proven difficult to obtain by other means. Our work suggests that this approach provides a potential means to target the role of Jak3 in autoimmunity and other disorders.

EXPERIMENTAL PROCEDURES

Jak3 Protein Production for X-ray Crystallography—Recombinant human Jak3(811–1103) C1040S/C1048S/D949A was expressed in SF9 cells as an N-terminal glutathione *S*-transferase fusion followed by a thrombin cleavage site. Insect cells were harvested after 72 h of growth postinfection. Surface cysteine mutants were introduced to decrease the DTT concentration necessary to minimize non-native disulfide formation at high protein concentration. The kinase-dead mutation (D949A) allowed for improved protein homogeneity and increased expression levels. Cell paste from 10 liters of culture (stored frozen at −80 °C) was thawed and resuspended in 1× TBS, 0.05% Tween 20, 250 mM NaCl, 10 mM DTT, 10% glycerol, 1 mM EDTA, 1 protease inhibitor tablet (Roche Applied Science, catalog no. 11873580001), and 10 μM Compound 4. The sample was sonicated with six 30-s pulses and centrifuged for 1 h using an SS-34 rotor at 17,000 rpm. The resulting supernatant was bound to GST affinity resin (GE Healthcare) at 4 °C. Thrombin was added to the slurry in the presence of 2.5 mM CaCl$_2$ overnight at 4 °C. The resin was subsequently washed with 1× TBS, 250 mM NaCl, 10% glycerol, 1 mM EDTA, 10 mM DTT, and 10 μM Compound 4 until thrombin-cleaved Jak3 was eluted. Pooled Jak3 was concentrated and further purified over an SEC Superdex 75 column (GE Healthcare) running in 20 mM Tris, pH 8.0, 250 mM NaCl, 10 mM DTT, 10% glycerol, and 10 μM Compound 4. Jak3-Compound 4 complex eluted at a corresponding molecular mass of ∼35,000 Da. Fractions containing Jak3 were pooled, concentrated to 10 mg/ml, and frozen at −80 °C. The Jak3 C1040S/C1048S/D949A was characterized by mass spectrometry and found to be unphosphorylated with one molecule of Compound 4 covalently attached. This sample was subsequently used in crystallographic experiments described below.

Position (in Jak3)	828	829	831	832	833	834	836	838	853	855	868	871	874	875	878	883	884	900	902	903
Jak3	**L**	**G**	**G**	**N**	**F**	**G**	**V**	**L**	**A**	**K**	**F**	**E**	**I**	**L**	**L**	**I**	**V**	**L**	**M**	**E**
Jak1	**L**	**G**	**G**	H	**F**	**G**	**V**	**L**	**A**	**K**	L	**E**	**I**	**L**	**L**	**I**	**V**	**L**	**M**	**E**
Jak2	**L**	**G**	**G**	**N**	**F**	**G**	**V**	M	**A**	**K**	F	**E**	**I**	**L**	**L**	**I**	**V**	**L**	**M**	**E**
Tyk2	**L**	**G**	**G**	H	**F**	**G**	**V**	**L**	**A**	**K**	W	**E**	**I**	**L**	**L**	**I**	I	**L**	**M**	**E**
Blk	**L**	**G**	**G**	Q	**F**	**G**	**V**	M	**A**	**K**	**F**	**E**	M	M	**L**	L	**V**	I	T	**E**
Bmx	**L**	**G**	**G**	Q	**F**	**G**	**V**	**L**	**A**	**K**	**F**	**E**	T	M	**L**	L	**V**	I	T	**E**
Btk	**L**	**G**	**G**	Q	**F**	**G**	**V**	Y	**A**	**K**	**F**	**E**	V	M	**L**	L	**V**	I	T	**E**
EGFR	**L**	**G**	**G**	A	**F**	**G**	**V**	K	**A**	**K**	I	**E**	V	M	V	V	C	**L**	T	Q
HER2	**L**	**G**	**G**	A	**F**	**G**	**V**	K	**A**	**K**	I	**E**	V	M	V	V	S	**L**	T	Q
HER4	**L**	**G**	**G**	A	**F**	**G**	**V**	K	**A**	**K**	**F**	**E**	**I**	M	M	L	**V**	**L**	T	Q
Itk	I	**G**	**G**	Q	**F**	**G**	**V**	**L**	**A**	**K**	**F**	**E**	V	M	**L**	L	**V**	**L**	F	**E**
Tec	**L**	**G**	**G**	L	**F**	**G**	**V**	**L**	**A**	**K**	**F**	**E**	V	M	**L**	L	**V**	I	T	**E**
Rlk/Txk	I	**G**	**G**	Q	**F**	**G**	**V**	**L**	**A**	**K**	**F**	**E**	V	M	**L**	L	**V**	I	T	**E**
Map2k7	M	**G**	**G**	T	C	**G**	**V**	K	**A**	**K**	I	D	V	V	S	I	**V**	I	**M**	**E**

Position (in Jak3)	904	905	906	907	908	909	912	940	945	947	948	953	954	956	965	966	967	968	969
Jak3	**Y**	**L**	**P**	**S**	**G**	**C**	**D**	**L**	**C**	**H**	**R**	**R**	**N**	**L**	**I**	**A**	**D**	**F**	**G**
Jak1	F	**L**	**P**	**S**	**G**	S	E	**L**	Y	**H**	**R**	**R**	**N**	**L**	**I**	G	**D**	**F**	**G**
Jak2	**Y**	L	**P**	Y	**G**	S	**D**	**L**	Y	**H**	**R**	**R**	**N**	**L**	**I**	G	**D**	**F**	**G**
Tyk2	**Y**	V	**P**	L	**G**	S	**D**	**L**	Y	**H**	**R**	**R**	**N**	**L**	**I**	G	**D**	**F**	**G**
Blk	**Y**	M	A	R	**G**	**C**	**D**	I	S	**H**	**R**	A	**N**	**L**	**I**	**A**	**D**	**F**	**G**
Bmx	**Y**	I	S	N	**G**	**C**	N	**L**	F	**H**	**R**	**R**	**N**	**L**	V	S	**D**	**F**	**G**
Btk	**Y**	M	A	N	**G**	**C**	N	**L**	F	**H**	**R**	**R**	**N**	**L**	V	S	**D**	**F**	**G**
EGFR	L	M	**P**	F	**G**	**C**	**D**	**L**	L	**H**	**R**	**R**	**N**	**L**	**I**	T	**D**	**F**	**G**
HER2	L	M	**P**	Y	**G**	**C**	**D**	**L**	L	**H**	**R**	**R**	**N**	**L**	**I**	T	**D**	**F**	**G**
HER4	L	M	**P**	H	**G**	**C**	E	**L**	L	**H**	**R**	**R**	**N**	**L**	**I**	T	**D**	**F**	**G**
Itk	F	M	E	H	**G**	**C**	**D**	**L**	V	**H**	**R**	**R**	**N**	**L**	V	S	**D**	**F**	**G**
Tec	F	M	E	R	**G**	**C**	N	**L**	F	**H**	**R**	**R**	**N**	**L**	V	S	**D**	**F**	**G**
Rlk/Txk	F	M	E	N	**G**	**C**	N	**L**	Y	**H**	**R**	**R**	**N**	**L**	**I**	S	**D**	**F**	**G**
Map2k7	L	M	-	G	T	**C**	K	**L**	V	**H**	**R**	S	**N**	**L**	F	C	**D**	**F**	**G**

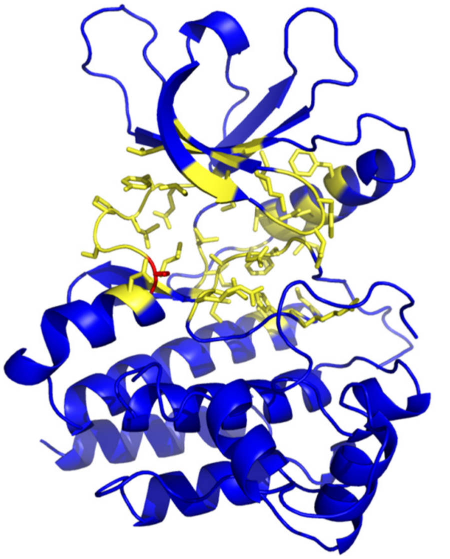

FIGURE 1. **Sequence conservation of human Janus kinase active sites and other kinases carrying a reactive thiol analogous to Cys-909 of Jak3.** Positions listed *above* are shown on the crystal structure of Jak3 in *yellow*. Cys-909 is highlighted in *red*.

Kinase Inhibition Assays—Wild-type Jak3 enzyme (amino acids 811–1103; expressed in SF9 cells with an N-terminal glutathione *S*-transferase (GST) tag) was purified by the same method as described above for the inactive C1040S/C1048S/D949A construct, except in the presence of a higher DTT concentration (40 mM). This enzyme (typically at concentrations of 2 nM) was mixed with 2 μM peptide substrate (biotin-TYR2;

sequence, Biotin-(Ahx)[2]-AEEEYFFLFA-amide) and 1 μM ATP (unless stated otherwise) at varying concentrations of inhibitor in reaction buffer: 50 mM MOPSO, pH 6.5, 10 mM $MgCl_2$, 2 mM $MnCl_2$, 2.5 mM DTT, 0.01% BSA, and 0.1 mM Na_3VO_4. After a 60-min incubation at room temperature, the reaction was quenched by the addition of EDTA (final concentration 100 μM) and developed by the addition of revelation reagents (final approximate concentrations: 30 mM HEPES, pH 7.0, 0.06% BSA, 0.006% Tween 20, 0.24 M KF, 80 ng/ml PT66K (europium-labeled anti-phosphotyrosine antibody, catalog no. 61T66KLB, Cisbio, Bedford, MA), and 3.12 μg/ml SAXL (Phycolink streptavidin-allophycocyanin acceptor, catalog no. PJ25S, Prozyme, San Leandro, CA)). The developed reaction was incubated in the dark either at 4 °C overnight or at room temperature for ~1 h and then read via a time-resolved fluorescence detector (Rubystar, BMG Labtech) using a 337-nm laser for excitation and emission wavelengths of 620 and 665 nm. Within the assay's linear range, acceptor fluorescence at 665 nm is directly related to phosphorylated product and used to calculate IC_{50} values. Typically, seven-point dilutions (5-fold; from 50 to 0.0032 μM) were used. IC_{50} value were calculated by fitting the following equation,

$$Y = Y_{\max} \times IC_{50}/(IC_{50} + [I]) \qquad \text{(Eq. 1)}$$

where [I] is total inhibitor concentration, Y is the percentage of activity (relative to that seen in no inhibitor control) at a given inhibitor concentration, and $Y_{\max}$ is the maximum activity generated in the absence of inhibitor. We estimated the precision of the Jak3 assay by calculating an intrarun minimum significant ratio (32, 33) of ~3. Purified Jak2 was purchased from Upstate/Millipore (catalog no. 14-640). Tyk2(880–1185) and Jak1(845–1142), both expressed in SF9 cells and purified in-house, were used in homogeneous time-resolved fluorescence kinase assays in the reaction buffer described above. Jak1 used substrate peptide biotin-TYR2, whereas Jak2 and Tyk2 used biotin-TYR1 (sequence, Biotin-(Ahx)-GAEEEIYAAFFA-COOH).

Jak3 Reversibility Experiments—To assess reversibility of inhibitor binding to Jak3, compounds were mixed with Jak3 (with or without 1× ATP) in assay buffer. Compounds were added at ≥5× Jak3 starting concentration. Starting inhibitor concentrations at ~IC_{90} were based on previous IC_{50} data generated by a similar reaction following a 30-min preincubation of enzyme and compound with or without ATP (IC_{90} ~10× IC_{50}). The samples were preincubated at room temperature for 30 min, followed by 400× dilution to reaction buffer in order to shift the equilibrium of inhibitor binding. Specifically, Compounds 1 and 4 were preincubated at 2 μM concentrations with 0.32 μM Jak3 in the absence of ATP and diluted 400-fold, where kinase reactions in 1 μM ATP were performed. Compounds 3 and 6 were preincubated at 2.8 and 15.2 μM concentrations, respectively with 0.32 μM Jak3 plus 10 μM ATP and diluted 400-fold, where kinase reactions in 10 μM ATP were performed. Jak3 kinase reactions were initiated using the assay conditions described above.

Jak3 Binding Kinetic Studies—Inhibitor association with Jak3 was determined by the loss of trFRET signal upon displacement of a fluorescent, reversible, active site probe labeled with Oregon Green-488 (2′,7′-difluoro-3′,6′-dihydroxy-3-oxo-*N*-(3-(3-(((6-oxo-4-(1H-pyrrolo[2,3-b]pyridin-3-yl)-1,6-dihydropyrimidin-2-yl)amino)methyl)phenoxy)propyl)-3H-spiro[isobenzofuran-1,9′-xanthene]-5-carboxamide). This probe was determined to bind to our Jak2 construct with K_d = 180 nM (data not shown). GST-Jak3 (Invitrogen, catalog no. PV3855) was premixed with terbium chelate-labeled anti-GST antibody (Invitrogen, catalog no. PV3550) in 50 mM HEPES, pH 7.5, 10 mM $MgCl_2$, 1 mM EGTA, and 0.01% Brij-35. Inhibitor was then added to the preformed Jak3-probe complex, and the decay of trFRET signal was measured on an Envision plate reader with excitation at 490 nm and emission at 520 nm at 2-min intervals for 1 h. Final concentrations were 1 nM GST-JAK3, 2 nM terbium anti-GST antibody, 200 nM labeled probe, and inhibitor concentrations of 0.00064, 0.0032, 0.016, 0.08, 0.4, 2, or 10 μM in a total volume of 40 μl. trFRET curves describing the disappearance of Jak3-probe complex were fit to a single exponential decay to determine k_{obs} and the change in signal $\Delta trFRET_{\text{tot}}$ at each inhibitor concentration.

There are two relevant binding mechanisms for analysis of k_{obs} and the change in amplitude. Mechanism 1 describes one-step reversible binding,

$$\text{Jak3} + \text{I} \overset{k_1}{\underset{k_2}{\leftrightarrow}} \text{Jak3-I}$$

Mechanism 1

where Jak3-I is the enzyme-inhibitor complex, and k_1 and k_2 are the rate constants for compound association and dissociation, respectively. In Mechanism 1, the observed rate at which Jak3-I is formed at any inhibitor concentration is described by the following.

$$k_{\text{obs}} = k_1[I] + k_2 \qquad \text{(Eq. 2)}$$

From a plot of k_{obs} *versus* [I], k_1 is determined from the slope, and k_2 is determined from the y intercept. Here, the binding amplitude is a function of the inhibitor concentration and its affinity.

$$\Delta\text{trFRET} = \frac{\Delta\text{trFRET}_{\text{tot}}[I]}{K_i + [I]} \qquad \text{(Eq. 3)}$$

For the sake of clarity, contributions of trFRET probe affinity and concentration to Equation 3 have been omitted. Although these are important for determining the absolute affinity of compounds, they are not important for the qualitative interpre-

---

[2] The abbreviations used are: Ahx, aminohexanoic acid; BLK, B lymphocyte kinase; BMX, bone marrow tyrosine kinase gene on chromosome X (also known as ETK); BTK, Bruton's tyrosine kinase; EGFR, epidermal growth factor receptor; FERM, four-point-one, ezrin, radixin, moesin; HER2, human epidermal growth factor receptor 2 (also known as ErbB2); HER4, human epidermal growth factor receptor 4 (also known as ErbB4); ITK, IL-2-inducible T-cell kinase; MAP2K7, mitogen-activated protein kinase kinase 7; RLK, resting lymphocyte kinase (also known as Txk); TEC, tyrosine kinase expressed in hematopoietic carcinoma; trFRET, time-resolved fluorescence resonance energy transfer; MOPSO, 3-morpholino-2-hydroxypropanesulfonic acid sodium salt; pSTAT, phosphorylated STAT; BisTris, bis(2-hydroxyethyl)iminotris(hydroxymethyl)methane; EPO, erythropoietin.

tations made to distinguish Mechanism 1 from Mechanism 2, below.

In the case of irreversible inhibitors, formation of a covalent enzyme-inhibitor complex occurs subsequent to binding as given by Mechanism 2,

$$\mathrm{Jak3} + \mathrm{I} \underset{k_2}{\overset{k_1}{\leftrightarrow}} \mathrm{Jak3\text{-}I} \underset{k_4}{\overset{k_3}{\leftrightarrow}} \mathrm{Jak3\text{-}I^*}$$

Mechanism 2

in which Jak3-I* is the covalent complex. Writing the rate equation for the disappearance of unbound Jak3 in Mechanism 2 and subsequent integration provides the following solution for k_{obs}.

$$k_{\mathrm{obs}} = \frac{k_1(k_3 + k_4)}{k_2 + k_3 + k_4}[\mathrm{I}] + \frac{k_2 k_4}{k_2 + k_3 + k_4} \quad \text{(Eq. 4)}$$

When the covalent complex is irreversible, k_4 is zero, and k_{obs} simplifies to the following.

$$k_{\mathrm{obs}} = \frac{k_1 k_3}{k_2 + k_3}[\mathrm{I}] \quad \text{(Eq. 5)}$$

Equations 4 and 5 both predict k_{obs} to be a linear function of [I] but are distinguished by Equation 5 having no y intercept. When Equation 5 is operative, the slope term $k_1k_3/(k_2 + k_3)$ is equivalent to k_{inact}/K_I, in which $k_{\mathrm{inact}} = k_3$ and $(k_2 + k_3)/k_1$ is K_I (which is distinct from $K_i = k_2/k_1$ for Mechanism 1). The term k_{inact}/K_I is commonly used to rank-order covalent inhibitors because it removes incubation time as a variable, unlike IC_{50} measurements. Note that binding progress curves for irreversible inhibitors obtain complete conversion to inhibitor-bound enzyme in cases where [I] ≥ [Jak3]. This feature distinguishes Mechanism 2 from Mechanism 1, where the extent of binding is sensitive to [I], as dictated by Equation 3. The concentration dependence of k_{obs} provides an apparent second-order rate constant regardless of whether Mechanism 1 or 2 is operative. Its interpretation as k_1 or as k_{inact}/K_I, respectively, can be distinguished kinetically by how the amplitude changes with concentration. This distinction is important because optimization of reversible inhibitors is through potency, typically driven by improvements in dissociation (k_2) alone, whereas optimization of irreversible inhibitors is through k_{inact}/K_I, which drives speed of interaction.

Cys Kinome Profiling—The 10 other protein kinases containing a cysteine in the residue analogous to Cys-909 in Jak3 were tested in a dedicated panel, without compound preincubation, under the same experimental conditions described for the Jak3 assay with the exception that ATP concentration was maintained near its K_m for each enzyme: BLK, EGFR, ErbB2, ErbB4, and Itk at 1 μM ATP; BTK, ITK, and MAP2K7 at 10 μM ATP; ETK and TEC at 100 μM ATP.

Kinome Profiling—trFRET-based binding displacement studies using active site probes were used to assess kinome selectivity of inhibitor molecules. The concentrations of components for each purified kinase were based on optimized conditions with ranges as follows: kinases (2–10 nM; Invitrogen), Oregon Green-labeled fluorescent probes (2× K_D of probe to the particular kinase; range of 6.25–200 nM; in-house/Invitrogen), terbium anti-His or anti-GST antibody (2 nM; Invitrogen). The reaction buffer contained 20 mM HEPES, pH 7.4, 10 mM $\mathrm{MgCl_2}$, 0.0075% Triton X-100, 0.1 mM $\mathrm{Na_3VO_4}$, 1 mM DTT. Compounds were typically tested from 0.0001 to 10 μM in 10× dilutions. Reactions were carried out in a 20-μl volume in PerkinElmer Life Sciences Proxiplate-plus 384-well white plates by combining kinase, probe, antibody, and test compound and then mixing and allowing the reaction to come to equilibrium (incubation of 2.5 h). trFRET was then measured on a PerkinElmer Envision plate reader (excitation at 340 nm; emission at 520 and 495 nm). Competition by the test compound *versus* the fluorescent probe for the ATP binding site of the kinase was quantified by calculating the IC_{50} value based on a four-parameter logistic curve fit.

Jak1 Cellular Assay; IL-6-induced pSTAT3 in TF-1 Cells—TF-1 cells were cultured in media for 18 h without GM-CSF prior to being plated in Alphaplate 384-well plates at 1×10^5 cells/well in 5 μl. Compound was added to cells (2.5 μl of 4× stock in 2% DMSO) and incubated for 30 min. Cells were then stimulated by adding 2.5 μl/well of 400 ng/ml (4× stock) IL-6 (R&D Systems catalog no. 206-IL/CF-50) and incubated for 30 min. Cells were lysed by adding 2.5 μl/well of 5× lysis buffer from the pSTAT3 kit, and plates were put on a shaker for 10 min (PerkinElmer Life Sciences catalog no. TGRS3S10K and bead kit 6760617M). Acceptor bead mix was made as per kit instructions, and 15 μl was added to each well and incubated on a shaker for 2 h at room temperature. Donor bead mix was prepared as per the kit instructions and added in a volume of 6 μl/well, and the plate was incubated on a shaker overnight at room temperature.

For all cell-based assays, plates were read on the EnVision reader (PerkinElmer Life Sciences), and EC_{50} values were obtained by plotting the percentage of control values in GraphPad Prism and using a non-linear curve fit to determine EC_{50}.

Jak2 Cellular Assay; EPO-induced pSTAT5 in UT-7/EPO Cells—UT7/EPO cells were cultured for 24 h without EPO and were plated in Alphaplate 384 plates at 1×10^5 cells/well in 5 μl. Compound was added to cells (2.5 μl of 4× stock in 2% DMSO) and incubated for 30 min. Cells were then stimulated by adding 2.5 μl/well of 4 nM (4× stock) EPO (Cell Sciences catalog no. CRE600B) and incubated for 20 min. Cells were lysed by adding 2.5 μl/well of 5× lysis buffer from the pSTAT5 kit, and plates were put on a shaker for 10 min (PerkinElmer Life Sciences catalog no. TGRS5S10K; bead kit catalog no. 6760617M). pSTAT5 was measured as described above for the IL-2 pSTAT3 assay, except pSTAT5 kits (PerkinElmer Life Sciences catalog no. TGRS5S10K) were used.

Jak3/Jak1 Cellular Assay; IL-2-induced pSTAT5 in T-blast Cells—T-blast cells were prepared from a LeukoPak and frozen. Cells were thawed and cultured for 24 h without IL-2 and were plated in Alphaplate 384 plates at 1×10^5 cells/well in 5 μl. Compound was added to cells (2.5 μl of 4× stock in 2% DMSO) and incubated for 30 min. Cells were then stimulated by adding 2.5 μl/well of 80 ng/ml (4× stock) IL-2 (R&D Systems catalog no. 202-IL-10) and incubated for 20 min. pSTAT5 was assessed as described above for the EPO assay.

Intact Mass Spectrometry—The LC-MS/MS system used consisted of a capillary pump HPLC with a temperature-controlled autosampler and an internal column oven coupled to a 6538 QTOF system (Agilent Technologies, Santa Clara, CA) with a dual-spray ESI source, using MassHunter software version B.03.01 (Agilent Technologies) for operation and data acquisition. For intact molecular weight measurements, 8 μl of sample in PBS buffer at 0.1 μg/ml was injected using an 8-μl sample loop onto a Vydac C4 300-Å column (1 mm × 15 cm, 5 μm; Nest Group, Southborough, MA). The column temperature was maintained at 30 °C, and separation was performed using a linear gradient from 30% B to 75% B over 20 min using mobile phase A (99:1 water/acetonitrile containing 0.09% formic acid and 0.01% trifluoroacetic acid (v/v)) and mobile phase B (99:1 acetonitrile/water, containing 0.09% formic acid and 0.01% trifluoroacetic acid (v/v)). The mass spectrometer was operated in a positive ion mode in the extended dynamic range of 2 GHz using the dual spray with a reference mass of 922.00979 Da. Data were acquired from 400 to 3200 m/z at 7.18 spectra/s using the following acquisition parameters on the electrospray ionization source: gas temperature = 350 °C, drying gas = 12 liters/min, nebulizer 60 p.s.i.g., VCap = 4500 V, fragmentor = 275 V, skimmer 85 V, Oct RF Vpp = 750 V. Spectra were processed using maximum entropy deconvolution (mass range 32,000–35,000 Da, mass step of 1.0, S/N 200, m/z range 950–1175 Da).

Protein Digestion for Mapping—JAK3 (0.1 mg/ml, 10 μl in 50 mM MOPSO, pH 6.5, 10 mM $MgCl_2$, 2 mM MnCl2, 2.5 mM DTT, 0.01% BSA, 0.1 mM Na_3VO_4, 5% DMSO buffer) in the presence and absence of Compound 3 was reduced by the addition of 20 mM DTT. Trypsin and Lys-C (Princeton Separations, Princeton, NJ) were both added at 1:20 (w/w), and samples were microwaved (CEM Corp., Matthews, NC) for 15 min at 55 °C, 50 watts. Digestion was cooled to room temperature, and 10 μl was immediately injected.

MS/MS Acquisition for Mapping—The LC-MS/MS system used consisted of a capillary pump HPLC with a temperature-controlled autosampler and an internal column oven (Waters, Milford, MA), using MassLynx software version 4.1 coupled to an LTQ-Orbitrap Velos Fourier transform mass spectrometer (Thermo Scientific, San Jose, CA) equipped with generation 2 ion optics (Velos Pro) and a heated electrospray ionization source, using Xcalibur software version 2.1.0 (Thermo Scientific) for operation and data acquisition. Peptides were eluted off of a Jupiter C18 300-Å column (0.5 mm × 15 cm, 5 μm; Phenomenex, Torrance, CA). The column temperature was maintained at 30 °C, and separation was performed using a linear gradient at 15 μl/min from 10% B to 45% B over 55 min using mobile phase A (water containing 0.1% formic acid and 0.02% trifluoroacetic acid v/v) and mobile phase B (acetonitrile, containing 0.1% formic acid and 0.02% trifluoroacetic acid v/v). The mass spectrometer was operated in a positive ion mode. The spray voltage was set at 3.8 kV with sheath gas set at 10. Data-dependent acquisition was performed by acquiring one full mass spectrum in FT mode (mass resolutions = 60,000) within an m/z range from 250 to 2000, followed by five MS/MS scans in the ion trap at a normal scan rate using an isolation width of 2.0 m/z. The top five most abundant precursor ions were each sequentially subjected to collision-induced dissociation. Dynamic exclusion was enabled with a mass width of ±0.25 ppm, a repeat count of 2, and exclusion duration of 15 s. Charge state screening was enabled. For collision-induced dissociation, the normalized collision energy was set to 35 with an activation Q of 0.25 and activation time of 30 ms. All MS/MS spectra were collected with an automatic gain control target ion setting of 10,000 ions.

Jak3 Crystallography and Structural Modeling—The Jak3 C1040S/C1048S/D949A and Compound 4 complex was crystallized in 25% PEG 3350, 0.2 M ammonium sulfate, and 0.1 M BisTris, pH 5.5, at 18 °C by vapor diffusion. The crystals were then cryoprotected using 20% glycerol plus mother liquor and frozen in liquid nitrogen.

X-ray diffraction data of Jak3 complexed to Compound 4 were collected at the Industrial Macromolecular Crystallography Association Collaborative Access Team beamline at the Advanced Photon Source (Argonne, IL). The data were processed with the HKL2000 suite of programs (34). The x-ray diffraction data are summarized in Table 7. The structure was solved using PHASER (35–37), using Protein Data Bank entry 1YVJ (20) as the search model. Refinement of the complex structure was conducted using REFMAC. Manual fitting of the model was completed with the program O (38) and examination of σA-weighted $2F_O - F_C$ and $F_O - F_C$ electron density maps. Two copies of Compound 4 (one per kinase domain) were modeled into unbiased experimental density using the program AFITT (OpenEye Scientific, Sante Fe, NM). Final refinement and water placement were conducted using the programs COOT and BUSTER and converged at an R_{cryst} of 20.7% (R_{free} = 25.1%), 39.67–1.8 Å (39, 40). MAESTRO (Glide; Schrödinger, Inc., New York (41)) was used to obtain covalent docking poses for Compound 3 using the protein crystal structure of Jak3 and Compound 4 as a reference.

RESULTS

Several families of non-covalent tricyclic inhibitors for JAKs have been described (42–44). Based on docking experiments in the available crystal structures of JAK family kinase domains and our previous work with tricyclic chemical series in the JAK family (44), we designed several covalent inhibitors for Jak3 (Fig. 2; Compounds 1–3). These molecules include three different reactive groups extending from the "imidazo" portion of the tricyclic moiety that binds to the familiar so-called "hinge region" of Janus kinases. Compound 1 contains a chloroacetamide group predicted to irreversibly interact with Cys-909, whereas Compounds 2 and 3 carry acrylamide-derived Michael acceptors (see supplemental Methods for chemical syntheses).

Compound 1 Shows Time-dependent, ATP-competitive Inhibition of Jak3—In contrast to two well known reversible JAK inhibitors (Compounds 5 and 6), we found that Compound 1 shows strong time-dependent inhibition in Jak3 enzyme assays (Fig. 3). Without preincubation of the compound with Jak3, moderate potency is achieved with Compound 1 (~0.6 μM) when 1 μM ATP is added to initiate the kinase reaction in the presence of substrate peptide (Fig. 3*a*). Extending the preincu-

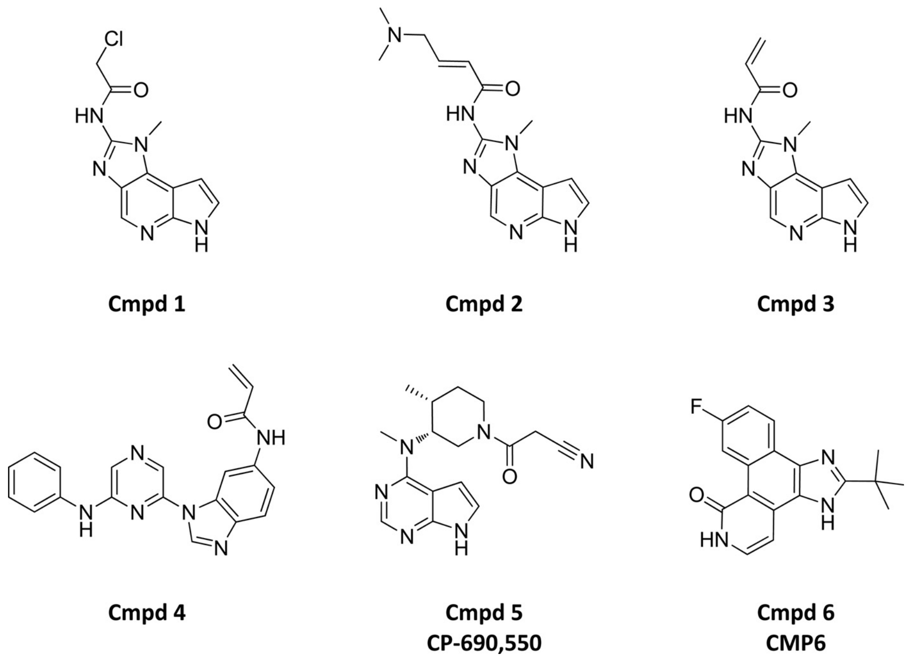

FIGURE 2. **Janus kinase inhibitors used in these studies.** *Cmpd*, compound.

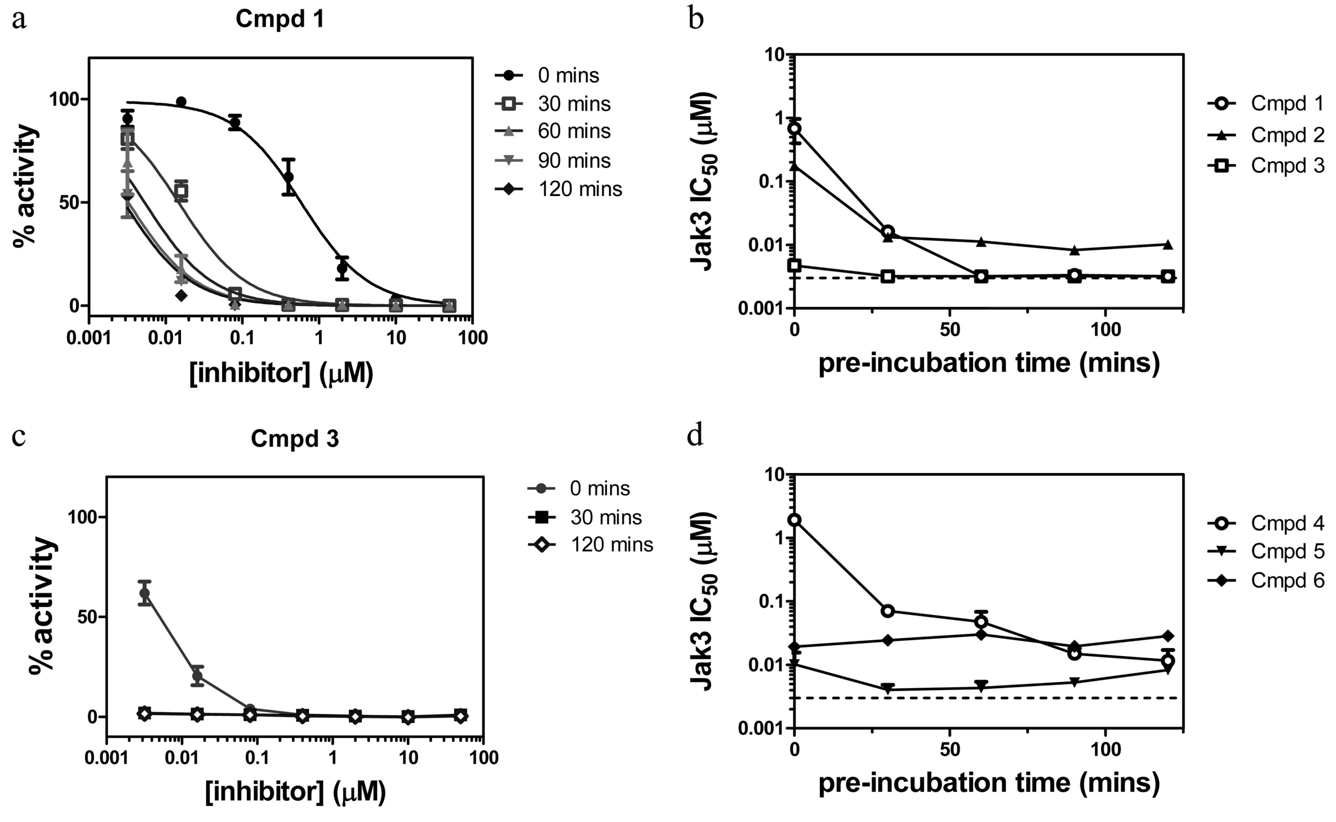

FIGURE 3. **Compounds (*Cmpd*) 1–4 show preincubation time-dependent changes in Jak3 inhibition.** Kinase reactions (60 min) were initiated by the addition of ATP (1 μM final) after the specified preincubation time with compounds and Jak3 in the presence of peptide substrate. *a*, inhibition curves using Compound 1. *b*, IC_{50} as a function of preincubation time for tricyclic compounds. *c*, inhibition curves using Compound 3. *d*, IC_{50} as a function of preincubation time for comparator compounds. Note that 0.003 μM is the lower limit of quantitation in the assay, as shown by the *dotted line* in *b* and *d*. *Error bars*, S.E.

bation time to 30 min greatly improved apparent potency to ~0.015 μM. With longer preincubation time, IC_{50} values of <3 nM are observed, which approaches the lower limit this assay can detect given the 2 nM enzyme concentration used. To further understand the differentiated mechanism of action of this compound, we compared Compound 1 with two previously described reversible JAK inhibitors, Compounds 5 and 6 (13, 23). In contrast to Compound 1, we found that Compounds 5 and 6 do not show this unusual time-dependent behavior of Jak3 inhibition (Fig. 3*d*). Within the ~3-fold precision of IC_{50}

TABLE 1

IC_{50} (μM) of inhibitors with varying order of addition and pre-incubation times

Compound	Compound + Jak3 + 1 μM ATP Pre-incubate Initiate reaction with peptide			Compound + Jak3 + 1 mM ATP Pre-incubate Initiate reaction with peptide			Compound + Jak3 + peptide Pre-incubate Initiate reaction with 1 mM ATP		
	Pre-incubation time (mins)								
	0	30	120	0	30	120	0	30	120
1 Tricycle	0.27	0.10	0.04	>50	>50	>50	>50	0.03	<0.003
4 Benzimidazole	1.4	0.6	0.5	>50	>50	>50	>50	0.1	0.02
5 CP-690,550	<0.003	<0.003	<0.003	4.7	3.8	3.3	5.4	4.8	4.0

values from our assay, no significant changes are observed with increasing preincubation times for Compounds 5 and 6, indicating they rapidly reach binding equilibrium on Jak3. From these results, we noted that the effects of Compound 1 are consistent with an inhibitor that binds slowly and/or has an irreversible step requiring a time scale similar to the length of the subsequent enzyme assays (~60 min) and can be contrasted to reversible Jak3 inhibitors.

To test whether Compound 1 was ATP-competitive, we ran Jak3 enzyme assays at a higher concentration of ATP (1 mM) and also varied the order of addition of ATP and peptide substrates used in the experiment (Table 1). IC_{50} values observed for Compound 5 increase >1000-fold regardless of incubation time or order of addition. This shift is consistent with that expected by the application of the Cheng-Prusoff equation using the ATP K_m we have measured for Jak3 (~1 μM; data not shown) and indicates ATP-competitive inhibition. We found our tricyclic inhibitor (Compound 1) was unable to significantly inhibit Jak3 ($IC_{50} > 50$ μM) when preincubated in the presence of 1 mM ATP. Interestingly, Compound 1 could inhibit Jak3 activity effectively if it was preincubated with enzyme in the presence of peptide for >30 min prior to the addition of 1 mM ATP. This suggests that Compound 1 competes with ATP. At high ATP concentrations, it is likely that Compound 1 does not have sufficient binding affinity to displace ATP from the Jak3 active site under these assay conditions. This is consistent with the absence of inhibition in preincubation experiments with 1 mM ATP but intermediate inhibition (0.3–0.040 μM) when preincubation mixtures include only 1 μM ATP (Table 1).

Styles *et al.* (45) at Cytopia described several benzimidazole-derived Jak3 inhibitors carrying Michael acceptors that were predicted to be covalent inhibitors. When comparing one of those compounds (Compound 4; see Fig. 2) with our tricyclic inhibitor, we see similar behavior in response to preincubation times and conditions (Fig. 3 and Table 1) although Compound 1 is somewhat more potent. Our subsequent tricycles, Compounds 2 and 3, show even more rapid time-dependent inhibition of Jak3 kinase activity (Fig. 3*b*). Compound 3 inactivates the enzyme with kinetics such that *without any preincubation*, it gives an IC_{50} of 5 nM in our assay, and with even brief preincubation before the addition of ATP, it reaches the lower limit of our assay conditions ($IC_{50} < 3$ nM).

Kinetics of Inhibitor Binding—Although IC_{50} measurements are often convenient to interpret, particularly when estimating selectivity between covalent and non-covalent interactions, the time dependence of IC_{50} values complicates the quantitation of drug-target interactions for covalent inhibitors. Also, the strong potency of Compound 3 observed in Jak3 activity assay IC_{50} values (Fig. 3*c*) limits its precise measurement. Therefore, we also measured the compounds' association kinetics with Jak3 through the displacement over time of a competitive trFRET-binding probe. Using the same trFRET signal, the K_d of this probe for Jak3 is 180 nM (data not shown).

Fig. 4*a* shows such data for Compound 3. We observed full displacement of the probe at all concentrations, except potentially 0.64 nM, which is substoichiometric to Jak3. This is characteristic of an irreversible inhibitor, Mechanism 2 (as described under "Experimental Procedures"). Values of k_{obs} from Fig. 4*a* were replotted *versus* inhibitor concentration (Fig. 4*c*), providing slope $= k_{inact}/K_I = 1.0 \times 10^7\ \text{M}^{-1}\ \text{min}^{-1}$ for Compound 3. Such analyses were performed on all compounds except for Compound 2 and enable compound ranking independent of preincubation time. They show Compound 3 to be nearly 200 times more optimized for Jak3 than Compound 4. In addition, the rank order of compounds from association studies

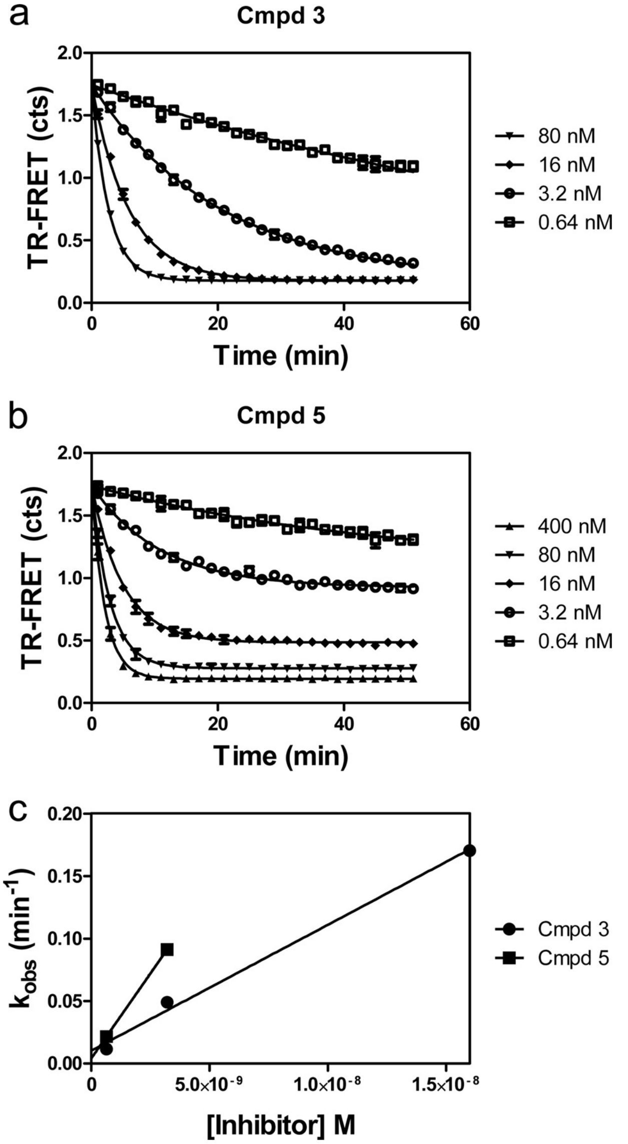

FIGURE 4. **Association kinetics of Jak3 inhibitors.** The association of inhibitor binding to Jak3 was monitored by the displacement of a trFRET probe. *a*, Compound (*Cmpd*) 3. *b*, Compound 5. Decay curves were fit to an exponential function from which values of k_{obs} and the amplitude changes at each inhibitor concentration were determined. *cts*, fluorescence counts. *c*, k_{obs} *versus* inhibitor concentration yields the association rate constant from the slope of the linear fit: Compound 3, $m = 1.0 \times 10^7$ M^{-1} min^{-1}; Compound 5, $m = 2.7 \times 10^7$ M^{-1} min^{-1}. Only k_{obs} values below 0.2 min^{-1} were used to ensure that rates had no contribution from dissociation of the trFRET probe.

TABLE 2

Kinetic binding studies of Jak3 inhibitors, association rate constant, and mode of interaction

Apparent association rate constants were determined by displacement of an active site trFRET probe as described in the legend of Fig. 4 and under "Experimental Procedures." Inhibitors on which $\Delta\text{trFRET}_{\text{tot}}$ is dependent on compound concentration are designated reversible, whereas those with constant $\Delta\text{trFRET}_{\text{tot}}$ are designated irreversible. Note that for reversible inhibitors, the association rate equals k_1, whereas for irreversible inhibitors, the association rate equals k_{inact}/K_I.

Compound	Apparent association rate constant	Observed binding mode
	M^{-1} min^{-1}	
1 (tricycle)	2.1×10^5	Irreversible
3 (tricycle)	1.0×10^7	Irreversible
4 (benzimidazole)	5.4×10^5	Irreversible
5 (CP-690,550)	2.7×10^7	Reversible
6 (CMP6)	1.3×10^7	Reversible

correlates well with the IC_{50}, cross-validating these two methods. All of the compounds tested that contain an apparent electrophilic group (Compounds 1, 3, and 4) demonstrated full displacement of the probe (not shown), and that behavior is summarized in Table 2.

Fig. 4*b* shows kinetic traces for Compound 5, where we note that the extent of probe displacement is proportional to inhibitor concentration. This is consistent with Mechanism 1 for reversible binding, as could be expected based on the lack of readily reactive groups in this molecule. Fitting the amplitude changes in Fig. 4*b* to Equation 2 yields K_i of 1.7 nM for Compound 5 (not shown), in agreement with the IC_{50} <0.003 μM in Table 1. Compound 6, which also lacks an apparent electrophile, demonstrated behavior similar to that of Compound 5 in its association kinetics and provided K_i of 49 nM (not shown), roughly similar to the 11 nM IC_{50} observed in the Jak3 activity assay (Table 3). Rate constants for Compounds 5 and 6 are included in Table 2, but because Mechanism 1 is operative, these values represent the association rate constant k_1.

Reversibility of Inhibitor Binding—To further assess whether our tricyclic compounds were irreversible inhibitors, we conducted an experiment to monitor potential recovery of activity after prebinding inhibitor to Jak3 and then shifting equilibrium by dilution to a state favoring inhibitor release (see "Experimental Procedures"; Fig. 5). The results indicate that Compound 6 is completely reversible and that the enzyme recovers full activity before the first time point in our experiment ($t_{1/2}$ for dissociation ≪5 min). However, essentially no recovery of Jak3 activity was observed for the tricyclic Compound 1 or 3 (Fig. 5) even after 80 min, which is similar to what was observed for Compound 4. These data suggest that these molecules are irreversible inhibitors of Jak3, although we cannot completely rule out the possibility they merely have a very long half-life on the enzyme (>3 h).

Mass spectrometry of Jak3 incubated in the presence of Compound 3 showed an increase of 241 Da compared with enzyme incubated with a DMSO control (Fig. 6*a*). This precisely matches the molecular mass of Compound 3 and strongly indicates that a covalent adduct was formed between Compound 3 and the enzyme. Furthermore, mass spectrometry mapping after protease digestion showed that the peptide containing Cys-909 was specifically modified by Compound 3 (Fig. 6*b*). Similar experiments with another tricyclic inhibitor, Compound 1, showed the expected change in intact molecular weight upon covalent modification of intact Jak3 (data not shown) following the loss of the chloride leaving group (228 Da). Notably, incubation with Compound 6, which we showed to be a reversible inhibitor earlier by enzyme kinetics, did not alter the molecular weight of Jak3 (Fig. 6*a*); nor did Compound 5 (data not shown).

In summary, our biochemical data indicate that our tricyclic inhibitors covalently modify Jak3 in an apparently irreversible manner and can be distinguished from earlier reversible Jak3 inhibitors, such as Compounds 5 and 6. In comparison with the benzimidazole Jak3 covalent inhibitor (Compound 4), we note that our lead tricycle (Compound 3) is a considerably more potent/rapid Jak3 inactivator.

TABLE 3

IC_{50} values (μM) for Janus family kinases

Preincubations contained compound, enzyme, and peptide substrate. All reactions were initiated by the addition of 1 μM ATP. Cmpd, compound.

	Preincubation time	IC_{50}					
		Cmpd 1(tricycle)	Cmpd 2 (tricycle)	Cmpd 3 (tricycle)	Cmpd 4 (benzimidazole)	Cmpd 5 (CP-690,550)	Cmpd 6 (CMP6)
	min				*μM*		
Jak1	0	5	6	4	>50	<0.003	<0.03
	120	8	11	6	>50	<0.003	0.01
Jak2	0	3.3	5	1.6	12	<0.003	<0.003
	120	4.3	5	1.6	48	<0.003	<0.003
Jak3	0	0.6	0.11	<0.003	0.5	<0.003	0.011
	120	<0.003	<0.007	<0.003	0.02	<0.003	0.011
Tyk2	0	46	>50	>50	3	0.05	0.005
	120	>50	>50	>50	6	0.02	0.011

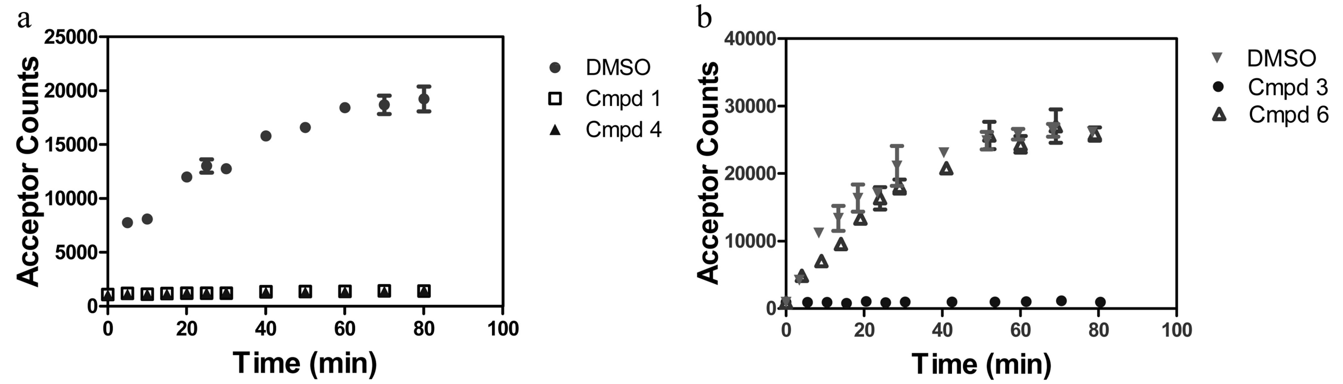

FIGURE 5. **Covalent inhibitors irreversibly inhibit Jak3.** *a*, Compounds (*Cmpd*) 1 and 4 were preincubated for 30 min at 2 μM concentrations with 0.32 μM Jak3 in the absence of ATP and diluted 400-fold, where kinase reactions in 1 μM ATP were performed. *b*, Compounds 3 and 6 were preincubated for 30 min at 2.8 and 15.2 μM concentrations, respectively, with 0.32 μM Jak3 plus 10 μM ATP and diluted 400-fold, where kinase reactions in 10 μM ATP were performed. *Error bars*, S.E.

Tricyclic Covalent Inhibitors Are Highly Selective for Jak3—Due to the presumed critical nature of the cysteine thiol for driving sustained interactions with the kinase, Jak3 covalent inhibitors would not be predicted to have significant activity against the other Janus kinases, which lack cysteine at this position (Fig. 1). We evaluated the potency of our covalent inhibitors in all JAK family kinases (Jak1, Jak2, Jak3, and Tyk2; see Table 3). Although some intrinsic binding to Jak1 and Jak2 with the tricyclic core is expected from previous results (44), we found that our tricyclic compounds gave IC_{50} values of >1 μM for Jak1, Jak2, and Tyk2. The lack of substantial increases in IC_{50} after a 2-h preincubation suggests that such interactions with these other isoforms are probably reversible in nature, consistent with the lack of the cysteine side chain in these isoforms. As expected, we found that the reversible inhibitors Compounds 5 and 6 inhibited all four Janus kinases with little selectivity among the family members (Table 3). We also probed the inhibition of the other 10 protein kinases that carry a cysteine in the analogous position in their active site (Table 4). Although some inhibition of these enzymes was observed, Compound 3 nevertheless exhibits strong selectivity for Jak3 compared with ITK (>100-fold) and with BTK and EFGR (>500-fold). The selectivity obtained for the benzimidazole covalent inhibitor (Compound 4) indicates more moderate selectivity.

We profiled our compounds in a kinome panel comprised of 78 representative protein kinases and found that our tricyclic inhibitors show excellent overall selectivity for Jak3 (Table 5). Compound 3, for example, binds Jak3 with a potency of 2 nM in the kinome panel. The next most potent interaction was with BTK at 1.3 μM. FGFR1 showed moderate inhibition at 3 μM, whereas 73 other kinase tested are >5 μM. Compound 4 showed a more moderate selectivity profile that probably reflects the less specific reversible interaction provided by its benzimidazole hinge-binding element.

Tricyclic Covalent Inhibitors Show Jak3 Selectivity in Cell-based Assays—Biochemical profiling uses isolated kinase domains separate from the regulatory machinery, binding partners, and other key features of how these proteins participate in a signaling pathway. To measure inhibition of JAKs in their native, cellular environment, we used a battery of cytokine-stimulated cell-based assays (Fig. 7 and Table 6). To interrogate common γ-chain signaling, we used an IL-2-stimulated T-blast assay that requires the activity of Jak3 and Jak1 to phosphorylate STAT5 (33). In this system, Compounds 1 and 2 show full inhibition of STAT5 phosphorylation with moderate potency (EC_{50} values of 1.3 and 0.5 μM, respectively). This inhibition is weaker than that of the reversible compound Compound 5, which showed EC_{50} of 48 nM. However, Compound 3, our most potent covalent tricyclic inhibitor when measured in isolated kinase domains, demonstrated even higher potency (19 nM) than Compound 5.

Importantly, the tricyclic compounds show essentially no activity in a Jak2-dependent cellular assay (EPO-stimulated phosphorylation of STAT5 in UT7 cells) even at compound concentrations greater than 50 μM (Fig. 7 and Table 6). In contrast, the reversible JAK inhibitors, Compounds 5 and 6, showed considerably less selectivity for Jak2, giving EC_{50} values

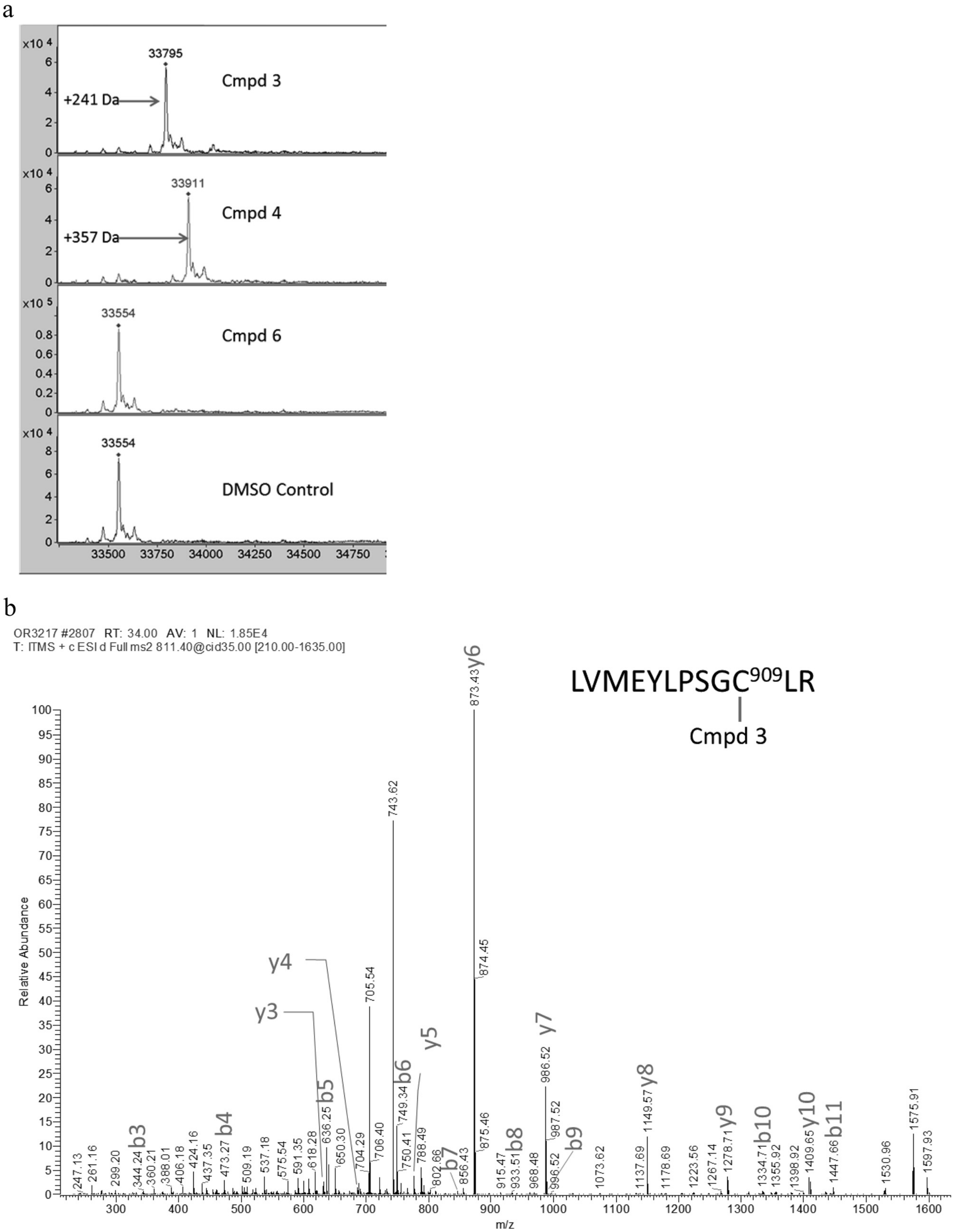

FIGURE 6. *a*, mass spectra of the Jak3 kinase domain shows that Compounds (*Cmpd*) 3 and 4 are covalent inhibitors. Jak3 was treated with inhibitor for 2 h (5-fold excess: 3 μM Jak3 and 15 μM inhibitor) in MOPSO kinase assay buffer in the absence of ATP at room temperature prior to mass spectrometry analysis. The known reversible inhibitor (Compound 6) does not modify the molecular weight. The predicted molecular mass for the Jak3 construct used carrying two phosphates is 33,550 Da. The predicted molecular mass of Compounds 3 and 4 is 241.3 and 356.4 Da, respectively. *b*, mass spectrometry mapping shows that Cys-909 is modified by Compound 3. Shown is the MS/MS spectrum (orbitrap/ion trap mode using an LTQ-Orbitrap) of peptide LVMEYLPSGCLR (*m/z* 811.40 {+2}) depicting modification of Cys-909 by Compound 3.

TABLE 4

The covalent inhibitors are selective for Jak3 among other kinases that carry homologous Cys

Jak3, EGFR BLK, EGFR, ErbB2, and ErbB4 were assayed using 1 μM ATP; BTK, ITK, and MAP2K7 were assayed using 10 μM ATP; ETK and TEC were assayed using 100 μM ATP (all near respective ATP K_m). IC$_{50}$ values were obtained with no preincubation in the absence of ATP.

	IC$_{50}$										
Compound	Jak3	Blk	Btk	EGFR	ErbB2/HER2	ErbB4/HER4	Etk/BMX	ITK	MAP 2K7	TEC	TXK/Rlk
						μM					
1	0.665	8.7	>10	>10	>10	6.4	>10	6.1	>10	3	7.5
3	0.007	2.6	14	11	>10	0.96	>10	0.83	>10	1	3.3
4	1.8	0.73	4.5	0.78	>10	0.91	>10	2.4	10	0.68	0.76
5	0.01	9.8	>10	33	>10	6	>10	49	18	0.64	>10
6	0.017	5.5	0.68	10	>10	3.1	>10	1.8	2.6	6.7	>10

at 1 and 0.25 μM, respectively, in the EPO-stimulated cellular assays. When compared in a Jak1 obligate assay (IL-6 phosphorylation of STAT3 in TF-1 cells), the covalent inhibitors also showed very little activity (EC$_{50}$ values of >17 μM), whereas the pan-JAK inhibitor Compound 5 showed a potent inhibition at 44 nM. Our *in vitro* enzyme and cellular data therefore strongly indicate a differentiated JAK inhibition profile for the tricyclic covalent inhibitors, which selectively inactivate Jak3 while sparing effects on Jak1 and Jak2. This cellular selectivity highlights the greater utility of Compound 3 over Compound 4 as a Jak3-specific inhibitor.

Structural Analysis of Jak3 Covalent Inhibitors—To better understand the interaction of covalent inhibitors with the Jak3 active site and how this exquisite Jak3 selectivity was obtained, we performed structural modeling with the tricyclic inhibitors and compared them with the co-crystal structure we obtained for Compound 4 in Jak3 (Fig. 8). This structure was solved and contained the Jak3 catalytic domain containing the mutations C1040S, C1048S, and D949A (submitted as PDB entry 4QPS). Mass spectrometry showed that, like the wild type, this inactive mutant protein also became covalently linked to Compound 4 (data not shown). Crystals were grown in 25% PEG 3350, 0.2 M ammonium sulfate (pH 5.5) over several days (see "Experimental Procedures" for details). They diffracted to 1.8 Å at a synchrotron source (Table 7).

In the structure of Compound 4 bound to Jak3, the acrylamide moiety is seen making a clear interaction with the sulfur atom in Cys-909. Continuous electron density between that side chain and the inhibitor is observed, as expected for covalent bonding between the inhibitor and protein (Fig. 8*a*). Although it is important to note that this is a product structure of the reaction of Compound 4 with the enzyme, we argue that a similar binding orientation with Compound 4 must have occurred prior to formation of covalent linkage. In this view, by positioning the acrylamide substitution off of the benzimidazole 6-position in close proximity to the sulfhydryl in Cys-909, Compound 4 would be placed in an orientation favorable for Michael addition of the corresponding thiol.

We modeled a tricycle into the binding site of Jak3 using our 4QPS x-ray structure as a reference. Based on the superposition of the Compound 3 model with the x-ray structure of Compound 4 (Fig. 8*c*), we found that the electrophile's trajectories were comparable. Because the orientations in Fig. 8 represent products after the covalent attachment for these compounds to Jak3, the greater reactivity of Compound 3 (larger k_{inact}/K_I and smaller Jak3 IC$_{50}$ values) compared with Compound 4 may stem from more favorable alignment in the active site prior to covalent attachment and/or greater affinity for reversible binding prior to nucleophilic attack by Cys-909. Although an x-ray structure would be helpful to confirm these observations, we note that in our model, the tricyclic core aligns with the kinase hinge with strong hydrogen bond distances to the backbone carbonyl of Glu-903 and backbone nitrogen of Leu-905. Additionally, in this model, the acrylamide carbonyl rotates to potentially form a stabilizing hydrogen bond to the backbone NH of Cys-909.

DISCUSSION

Tyrosine phosphorylation of STAT molecules by Janus kinase family members is a key step in numerous pathways of cytokine and proliferative signaling (3, 5, 46, 47). The JAKs represent attractive targets for therapeutic intervention in numerous human disease areas, including autoimmunity/inflammation, myeloproliferative disorders, and cancer. As such, compounds that inhibit or modulate their activity represent a considerable opportunity to improve patients' lives (for recent reviews, see Refs. 15 and 48).

Because of the high structural similarity of the four JAK enzymes, a key challenge in such strategies is the development of selective compounds that can target a particular Janus kinase isoform while avoiding inhibition of others that may lead to unacceptable side effects. A strong case can be made for therapeutics specifically targeting Jak3. Its expression is the most limited of the JAKs, chiefly in the hematopoietic cells (49) that play a central role in autoimmunity. Furthermore, inhibition of Jak3 would not be expected to impact the antiviral pathways such as IFN-α (which signals by Jak1 and Tyk2) that may otherwise limit use of JAK inhibitors for chronic diseases. Because of its role in several physiologically essential processes, such as erythropoiesis and neutrophil function (5, 50–52), avoiding inhibition of Jak2 is particularly desirable. Clinical results indicate that anemia could be potentially dose-limiting for JAK inhibitors with insufficient selectivity over Jak2 (53, 54). Therefore, specifically targeting Jak3 may improve safety margins, although the consequences of long term blockade of Jak3 in the absence of other JAKs are unknown.

Here, we have characterized the *in vitro* inhibition properties of several compounds that achieve Jak3 selectivity through the covalent interaction with a Jak3 active site cysteine not present in the other family members. As described above, we found that these compounds display time-dependent inhibition of Jak3 but not of other JAKs (Fig. 3 and Table 3). Like the other JAK inhibitors examined, their binding was influenced by the concentration of nucleotide and is therefore ATP-competitive

TABLE 5

Kinome selectivity of JAK inhibitors

trFRET competition binding IC$_{50}$ values (μM) are shown. ND, not determined. Cmpd, compound.

Kinase	IC$_{50}$				
	Cmpd 1	Cmpd 3	Cmpd 4	Cmpd 5	Cmpd 6
			μM		
ACVR1	>10	>10	2.7	9.4	>10
Abl	>10	>10	3.5	>10	>10
Akt1	ND	>10	>10	ND	>10
ALK	>10	>10	>10	>10	>10
Aurora1	>10	>10	6.7	>10	0.30
Aurora2	>10	>10	>10	>10	>10
BRAF	>10	>10	>10	>10	>10
BTK	>10	1.25	0.64	>10	>10
CAMK1D	>10	>10	>10	6.7	>10
CAMK2A	>10	>10	>10	>10	>10
CAMKK2	8.4	>10	>10	>10	>10
CDK11	>10	>10	>10	>10	>10
CDK2	ND	>10	>10	ND	>10
CDK7	9.5	>10	>10	>10	>10
CDK8	8.5	>10	3.8	5.9	>10
CDK9	>10	>10	>10	>10	>10
Ck1α1	>10	>10	7.6	>10	>10
CLK2	>10	>10	3.9	4.9	>10
cMET	7.0	>10	>10	>10	>10
CSF1R	>10	>10	>10	>10	>10
DDR1	>10	>10	>10	>10	>10
Dyrk1A	>10	>10	>10	>10	>10
DYRK1B	>10	>10	8.8	9.63	>10
Erk2	ND	>10	>10	ND	1.47
FAK	>10	>10	>10	>10	1.9
FGFR1	>10	3.1	4.4	>10	>10
Flt1	>10	>10	0.55	>10	>10
Fyn	>10	ND	0.66	>10	>10
GRK5	7.7	9.4	>10	>10	2.5
Gsk3a	>10	>10	5.0	>10	>10
Gsk3b	>10	>10	7.4	>10	>10
IGF1R	>10	>10	>10	>10	>10
IKKe	>10	>10	>10	>10	0.35
InsR	>10	>10	>10	>10	>10
JAK2	>10	>10	>10	0.017	0.010
JAK3	0.099	0.002	0.30	0.017	0.072
JNK1	>10	>10	>10	>10	0.037
JNK2	>10	>10	>10	>10	0.20
Kdr	7.3	ND	0.55	4.0	6.3
Lck	>10	>10	4.5	>10	>10
LTK	7.3	5.6	9.2	3.3	0.11
MAP2K3	>10	>10	>10	ND	>10
MAP3K10	>10	>10	>10	>10	>10
MAP4K2	5.1	7.4	>10	>10	10.0
MAP4K4	>10	>10	8.1	>10	3.4
MEK1	5.0	>10	9.6	>10	0.45
MEK2	>10	>10	>10	>10	2.0
MST1	>10	>10	>10	>10	0.078
Nek2	>10	>10	>10	>10	>10
p38α	>10	>10	>10	>10	>10
PAK4KD	>10	>10	>10	>10	>10
PDGFRB	>10	>10	>10	>10	>10
Pim1	>10	>10	7.9	>10	1.6
Pim2	ND	>10	>10	>10	5.1
PKA	>10	>10	>10	7.8	3.9
PKCθ	>10	>10	>10	7.8	3.2
PKCζ	ND	>10	>10	>10	>10
PKG1A	>10	>10	>10	4.2	>10
Plk3	ND	>10	1.5	ND	>10
Prkcn	>10	>10	>10	>10	0.27
RET	8.0	7.8	>10	>10	0.73
Rock1	>10	>10	>10	1.7	0.48
Rock2	>10	>10	>10	1.2	>10
Rsk2	>10	>10	>10	>10	2.7
SGK1	>10	>10	>10	>10	1.8
Src	ND	>10	0.98	ND	>10
STK16	ND	>10	1	>10	>10
STK33	0.66	7.1	>10	>10	0.099
Syk	>10	>10	>10	>10	>10
TAOK2	>10	>10	>10	>10	>10
TBK1	>10	>10	>10	>10	0.70
TNK2	>10	>10	4.7	>10	0.51
TrkA	>10	>10	>10	>10	>10
TrkB	>10	>10	>10	>10	4.4
TrkC	>10	>10	>10	>10	9.1
TYRO3	>10	>10	>10	>10	>10
Wee1	9.8	>10	7.8	>10	>10
Zipk	6.3	>10	2.8	>10	0.002

(Table 1). This is consistent with the binding poses modeled for the tricyclic inhibitors and with the binding mode in the Jak3 active site observed for Compound 4 by crystallography (Fig. 8). In our crystal structure, a covalent interaction is observed between the terminal electrophile and the side chain of Cys-909. We found that, in contrast to the other well known Jak3 inhibitors (Compounds 5 and 6), our tricyclic compounds are effectively irreversible inhibitors of Jak3 (Figs. 4–6).

Although the presence of cysteine residues in this area of kinase active sites is relatively rare, there are several other tyrosine kinases that carry a thiol in a position analogous to that of Cys-909 of Jak3 (BLK, BMX, BTK, EGFR, HER2, HER4, ITK, RLK, and TEC) as well as one serine-threonine kinase (MAP2K7) (Fig. 1). These include enzymes that may be good targets for oncology (EGFR, HER2, and BLK) and immunological diseases (BTK, ITK, and TEC). Several inhibitors directed toward EGFR and BTK in this manner have been described (29, 55–59), and there is resurgent interest in covalent inhibitors of kinases (31, 60). Although the potential for cross-reactivity with thiol-directed inhibitors exists, there are other differences in the active site sequences of kinases carrying cysteine at this position (Fig. 1). This suggests that optimization of intrinsic (non-covalent) affinity of the inhibitor for the target kinase through improved interactions of the hinge-binding region and other inhibitor elements could introduce the necessary specificity to target particular kinases.

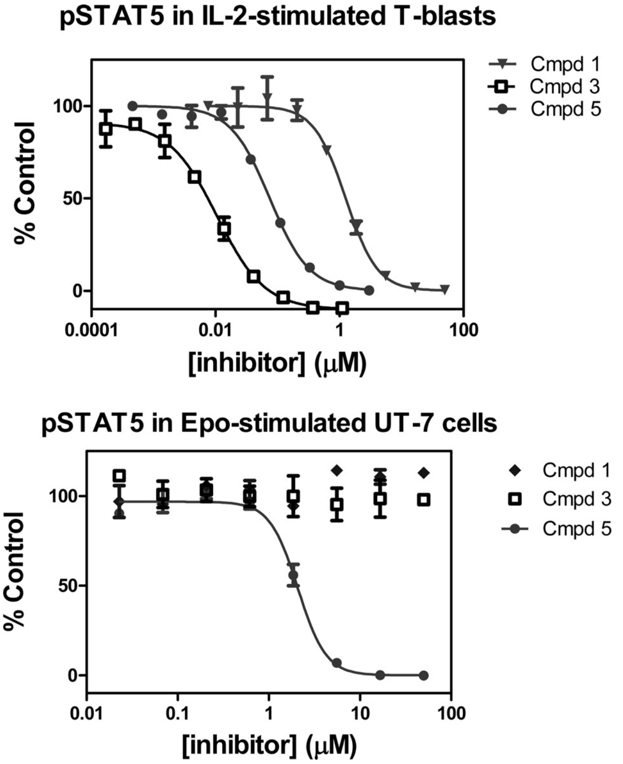

FIGURE 7. **Cellular activity of Jak3 inhibitors.** *Upper panel*, phosphorylation of STAT5 (*pSTAT5*) in IL-2-stimulated T-blasts (dependent on signaling from both Jak1 and Jak3). *Lower panel*, phosphorylation of STAT5 in EPO-stimulated UT-7 cells (dependent on signaling from Jak2). Covalent tricyclic compounds (Compounds (*Cmpd*) 1 and 3) are inactive (>50 μM) in this assay. *Error bars*, S.E.

We found that the favorable selectivity for JAKs that is imparted by certain tricyclic hinge-binding cores (44) could drive strong Jak3 selectivity if we added a reactive electrophile in the right location. Our inhibition data with other Cys-containing kinases (EGFR, ITK, BTK, etc.) show favorable selectivity ratios for our covalent inhibitors compared with Jak3, and we also observed good selectivity among more than 70 other kinases. The specificity of the tricyclic compounds shown herein for Jak3 is almost certainly driven in part by non-covalent interactions with Jak3 prior to covalent attack. We suspect that the tricycles probably have reversible affinity for the Jak3 active site in the 1–10 μM range, similar to the potency observed for these molecules in Jak1 and Jak2 (see Table 3), where no covalent bond can be formed. If, during reversible binding, the reactive group is brought into close proximity to Cys-909 for efficient covalent attack, even modest initial affinity would appear to drive rapid inactivation of Jak3. Thus, we conclude that our tricyclic core provides the correct balance of hinge hydrogen bond interactions with a suitable geometric approach to the target Cys-909 with a reactive moiety.

We observed that tricyclic compounds also carried strong selectivity within the JAK family for Jak3, both in enzyme assays with isolated kinases domains of Jak1, Jak2, and Tyk2 and in a battery of cell-based assays (Fig. 7). We note that the full inhibition of STAT5 phosphorylation in the IL-2 cell-based assay in T-blasts suggest that Jak3 inhibition alone (in the absence of appreciable Jak1 inhibition) is sufficient to block downstream signaling. This is consistent with a report by Liu *et al.* (61) who concluded from cell transfection experiments that both Jak1 and Jak3 were essential to achieving STAT phosphorylation in response to IL-2. Our result using native Jak3/IL-2 signaling in T-cells is in contrast to results described previously in U4C epithelial cells (62), where only partial effects on the level of STAT5 phosphorylation in response to IL-2 were observed using "kinase-dead" Jak3. We speculate the apparent differences may be due to the nature of the epithelial cell line used and the manner in which Jak3 was exogenously expressed in those experiments or that the K855A mutation used may not completely abrogate kinase activity.

A potential challenge with the use of covalent inhibitors carrying Michael acceptors lies in their potential reactivity with

TABLE 6

EC_{50} (μM) of Jak3 inhibitors in cell-based assays

ND, not determined. Cmpd, compound.

Assay	Cmpd 1 (tricycle)	Cmpd 2 (tricycle)	Cmpd 3 (tricycle)	Cmpd 4 (benzimidazole)	Cmpd 5 (CP-690,550)	Cmpd 6 (CMP6)
	EC_{50}					
				μM		
IL-6 pSTAT3 TF-1 cells (Jak1)	23	>50	17	19	0.044	ND
Epo pSTAT5 UT-7 cells (Jak2)	>50	>50	>50	>50	1.1	0.25
IL-2 pSTAT5 T-blasts (Jak1 and Jak3)	1.26	0.51	0.019	4.9	0.048	0.040

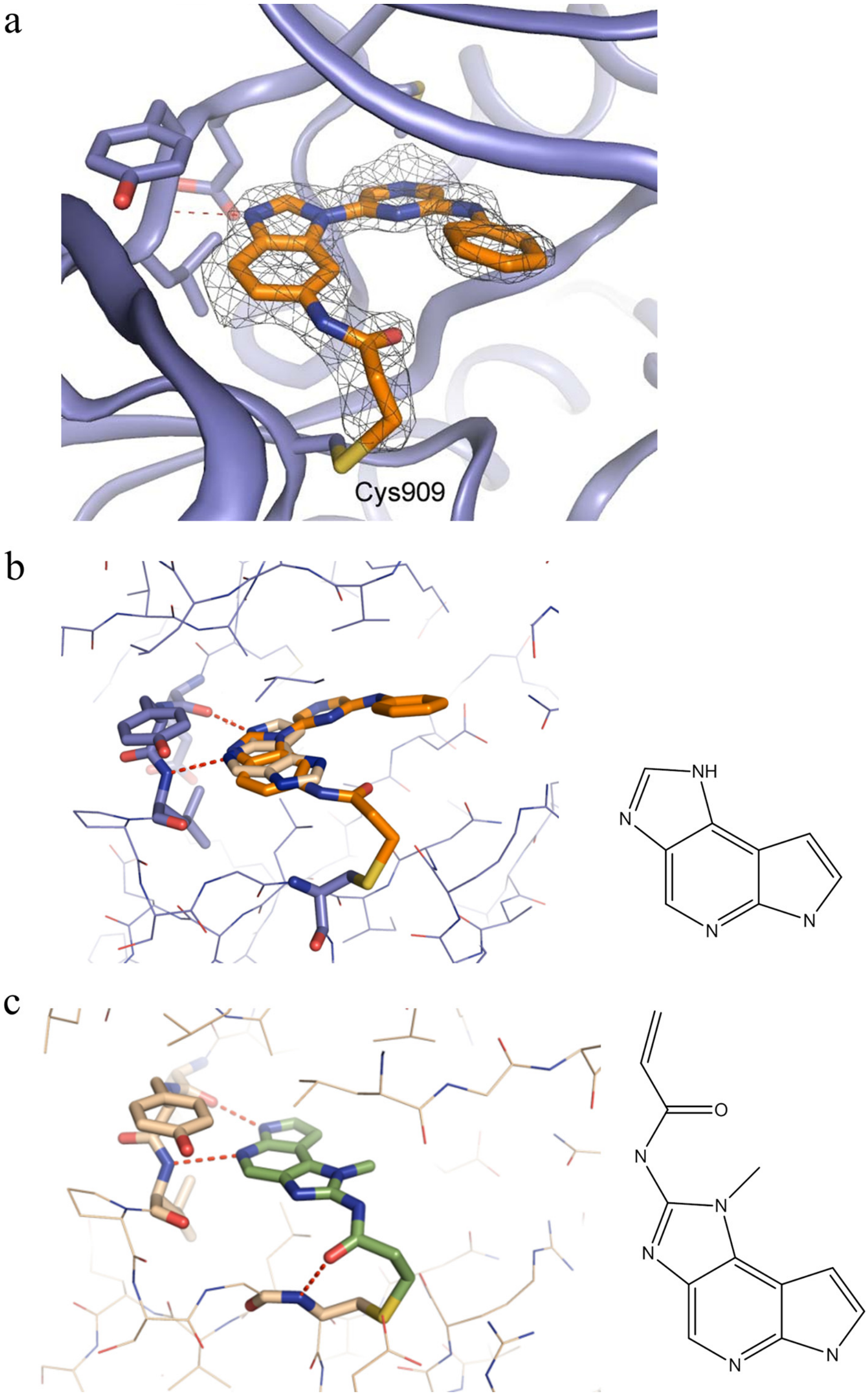

FIGURE 8. *a*, crystal structure of Compound 4 covalently bound to Jak3 (monomer C). Electron density from $F_O - F_C$ maps is shown contoured at 2σ. *b*, x-ray structure of Compound 4 (*dark orange*) and Jak3 overlaid with tricyclic core (*light orange*) modeled into the Jak3 active site. The structure of basic tricyclic core is shown on the *right*. *c*, Compound 3 modeled into Jak3 using a covalent docking method from the program Glide using 4QPS monomer C as a reference model (41).

additional proteins (63, 64). However, a number of covalent kinase inhibitors targeting EGFR or BTK have recently advanced to clinical testing, and, to the surprise of many, significant non-mechanistic adverse events have not been observed. Our *in vitro* data indicate that the acrylamide moiety of Compound 3 is not a highly non-selective modifier of thiols; mass spectrometry data show only one addition of Compound 3 despite the presence of other surface cysteines (Cys-1040 and -1048) in the Jak3 used for the experiment (Fig. 6). Although we do not underplay concerns about the potential reactivity of such molecules, we see potential for covalent inhibition of Jak3 in targeting diseases mediated for this important kinase. The covalent tricycles described here represent a good start to such efforts. However, we have not been able to obtain favorable

TABLE 7

Crystallographic statistics for Jak3 complexed to Compound 4

Parameter	Value
Protein Data Bank entry	4QPS
Data collection	
Resolution (Å)	39.67–1.8
Space group	$P2_1$
Unit cell lengths (a, b, c) (Å)	79.5, 43.9, 81.7 $\beta = 115.26$
Unique reflections	47056
Overall statistics (highest shell (Å))	
R_{sym} (%)	0.064 (0.25)
I/σ	16.0 (5.0)
Data completeness (%)	98.6 (97.6)
Mean multiplicity	3.5 (3.3)
Wilson plot B-or (Å^2)	24.5
Refinement	
Reflections used in refinement	47010
R_{cryst} (%)	20.7
R_{free} (%)	25.1
Root mean square deviations, bond lengths (Å)/bond angles (degrees)	0.010/1.04
Ramachandran plot (% most favored and additionally allowed residues)	97.2/2.2

pharmacokinetics with these compounds (data not shown) to extend their use as *in vivo* tools. Given the improvements in selectivity for Jak3 signaling that we observed in cell-based assays over previous molecules, our inhibitors could be valuable *in vitro* tool compounds to investigate the molecular and physiological consequences of Jak3-specific inhibition.

Acknowledgments—We thank Robert Talanian and Neil Wishart of AbbVie for helpful discussions; Andrew Gagnon, Ramkrishna Sadhukhan, Patrick Betschmann, David Borhani, Lori Dowding, Eric Dominguez, Dawn George, Qing Yu Lang, Silvino Sousa, Paul Richardson, and other members of the AbbVie JAK project team for additional efforts; and Kent Stewart of AbbVie for helpful discussions and critical reading of the manuscript.

REFERENCES

1. Darnell, J. E., Jr. (1997) STATs and gene regulation. *Science* **277,** 1630–1635
2. Horvath, C. M. (2000) STAT proteins and transcriptional responses to extracellular signals. *Trends Biochem. Sci.* **25,** 496–502
3. Yamaoka, K., Saharinen, P., Pesu, M., Holt, V. E., 3rd, Silvennoinen, O., and O'Shea, J. J. (2004) The Janus kinases (Jaks). *Genome Biol.* **5,** 253
4. Langrish, C. L., McKenzie, B. S., Wilson, N. J., de Waal Malefyt, R., Kastelein, R. A., and Cua, D. J. (2004) IL-12 and IL-23: master regulators of innate and adaptive immunity. *Immunol. Rev.* **202,** 96–105
5. Murray, P. J. (2007) The JAK-STAT signaling pathway: input and output integration. *J. Immunol.* **178,** 2623–2629
6. Watford, W. T., Hissong, B. D., Bream, J. H., Kanno, Y., Muul, L., and O'Shea, J. J. (2004) Signaling by IL-12 and IL-23 and the immunoregulatory roles of STAT4. *Immunol. Rev.* **202,** 139–156
7. Darnell, J. E., Jr., Kerr, I. M., and Stark, G. R. (1994) Jak-STAT pathways and transcriptional activation in response to IFNs and other extracellular signaling proteins. *Science* **264,** 1415–1421
8. Shuai, K., Ziemiecki, A., Wilks, A. F., Harpur, A. G., Sadowski, H. B., Gilman, M. Z., and Darnell, J. E. (1993) Polypeptide signalling to the nucleus through tyrosine phosphorylation of Jak and Stat proteins. *Nature* **366,** 580–583
9. Harpur, A. G., Andres, A. C., Ziemiecki, A., Aston, R. R., and Wilks, A. F. (1992) JAK2, a third member of the JAK family of protein tyrosine kinases. *Oncogene* **7,** 1347–1353
10. Wilks, A. F., Harpur, A. G., Kurban, R. R., Ralph, S. J., Zürcher, G., and Ziemiecki, A. (1991) Two novel protein-tyrosine kinases, each with a second phosphotransferase-related catalytic domain, define a new class of protein kinase. *Mol. Cell Biol.* **11,** 2057–2065
11. Changelian, P. S., Moshinsky, D., Kuhn, C. F., Flanagan, M. E., Munchhof, M. J., Harris, T. M., Whipple, D. A., Doty, J. L., Sun, J., Kent, C. R., Magnuson, K. S., Perregaux, D. G., Sawyer, P. S., and Kudlacz, E. M. (2008) The specificity of JAK3 kinase inhibitors. *Blood* **111,** 2155–2157
12. Thompson, J. E. (2005) JAK protein kinase inhibitors. *Drug News Perspect.* **18,** 305–310
13. Changelian, P. S., Flanagan, M. E., Ball, D. J., Kent, C. R., Magnuson, K. S., Martin, W. H., Rizzuti, B. J., Sawyer, P. S., Perry, B. D., Brissette, W. H., McCurdy, S. P., Kudlacz, E. M., Conklyn, M. J., Elliott, E. A., Koslov, E. R., Fisher, M. B., Strelevitz, T. J., Yoon, K., Whipple, D. A., Sun, J., Munchhof, M. J., Doty, J. L., Casavant, J. M., Blumenkopf, T. A., Hines, M., Brown, M. F., Lillie, B. M., Subramanyam, C., Shang-Poa, C., Milici, A. J., Beckius, G. E., Moyer, J. D., Su, C., Woodworth, T. G., Gaweco, A. S., Beals, C. R., Littman, B. H., Fisher, D. A., Smith, J. F., Zagouras, P., Magna, H. A., Saltarelli, M. J., Johnson, K. S., Nelms, L. F., Des Etages, S. G., Hayes, L. S., Kawabata, T. T., Finco-Kent, D., Baker, D. L., Larson, M., Si, M. S., Paniagua, R., Higgins, J., Holm, B., Reitz, B., Zhou, Y. J., Morris, R. E., O'Shea, J. J., and Borie, D. C. (2003) Prevention of organ allograft rejection by a specific Janus kinase 3 inhibitor. *Science* **302,** 875–878
14. Kudlacz, E., Perry, B., Sawyer, P., Conklyn, M., McCurdy, S., Brissette, W., Flanagan And, M., and Changelian, P. (2004) The novel JAK-3 inhibitor CP-690550 is a potent immunosuppressive agent in various murine models. *Am. J. Transplant.* **4,** 51–57
15. O'Shea, J. J., Kontzias, A., Yamaoka, K., Tanaka, Y., and Laurence, A. (2013) Janus kinase inhibitors in autoimmune diseases. *Ann. Rheum. Dis.* 10.1136/annrheumdis-2012-202576
16. Scott, L. J. (2013) Tofacitinib: a review of its use in adult patients with rheumatoid arthritis. *Drugs* **73,** 857–874
17. Simmons, D. L. (2013) Targeting kinases: a new approach to treating inflammatory rheumatic diseases. *Curr. Opin. Pharmacol.* **13,** 426–434
18. Gaestel, M., Kotlyarov, A., and Kracht, M. (2009) Targeting innate immunity protein kinase signalling in inflammation. *Nat. Rev. Drug Discov.* **8,** 480–499
19. Ghoreschi, K., Laurence, A., and O'Shea, J. J. (2009) Janus kinases in immune cell signaling. *Immunol. Rev.* **228,** 273–287
20. Boggon, T. J., Li, Y., Manley, P. W., and Eck, M. J. (2005) Crystal structure of the Jak3 kinase domain in complex with a staurosporine analog. *Blood* **106,** 996–1002
21. Chen, J. J., Thakur, K. D., Clark, M. P., Laughlin, S. K., George, K. M., Bookland, R. G., Davis, J. R., Cabrera, E. J., Easwaran, V., De, B., and George Zhang, Y. (2006) Development of pyrimidine-based inhibitors of Janus tyrosine kinase 3. *Bioorg. Med. Chem. Lett.* **16,** 5633–5638
22. Clark, M. P., George, K. M., Bookland, R. G., Chen, J., Laughlin, S. K., Thakur, K. D., Lee, W., Davis, J. R., Cabrera, E. J., Brugel, T. A., VanRens, J. C., Laufersweiler, M. J., Maier, J. A., Sabat, M. P., Golebiowski, A., Easwaran, V., Webster, M. E., De, B., and Zhang, G. (2007) Development of new pyrrolopyrimidine-based inhibitors of Janus kinase 3 (JAK3). *Bioorg. Med. Chem. Lett.* **17,** 1250–1253
23. Lucet, I. S., Fantino, E., Styles, M., Bamert, R., Patel, O., Broughton, S. E., Walter, M., Burns, C. J., Treutlein, H., Wilks, A. F., and Rossjohn, J. (2006) The structural basis of Janus kinase 2 inhibition by a potent and specific pan-Janus kinase inhibitor. *Blood* **107,** 176–183
24. Thompson, J. E., Cubbon, R. M., Cummings, R. T., Wicker, L. S., Frankshun, R., Cunningham, B. R., Cameron, P. M., Meinke, P. T., Liverton, N., Weng, Y., and DeMartino, J. A. (2002) Photochemical preparation of a pyridone containing tetracycle: a Jak protein kinase inhibitor. *Bioorg. Med. Chem. Lett.* **12,** 1219–1223
25. Williams, N. K., Bamert, R. S., Patel, O., Wang, C., Walden, P. M., Wilks, A. F., Fantino, E., Rossjohn, J., and Lucet, I. S. (2009) Dissecting specificity in the Janus kinases: the structures of JAK-specific inhibitors complexed to the JAK1 and JAK2 protein tyrosine kinase domains. *J. Mol. Biol.* **387,** 219–232
26. Argiriadi, M. A., Goedken, E. R., Banach, D., Borhani, D. W., Burchat, A., Dixon, R. W., Marcotte, D., Overmeyer, G., Pivorunas, V., Sadhukhan, R., Sousa, S., Moore, N. S., Tomlinson, M., Voss, J., Wang, L., Wishart, N., Woller, K., and Talanian, R. V. (2012) Enabling structure-based drug de-

sign of Tyk2 through co-crystallization with a stabilizing aminoindazole inhibitor. *BMC Struct. Biol.* **12,** 22

27. Chrencik, J. E., Patny, A., Leung, I. K., Korniski, B., Emmons, T. L., Hall, T., Weinberg, R. A., Gormley, J. A., Williams, J. M., Day, J. E., Hirsch, J. L., Kiefer, J. R., Leone, J. W., Fischer, H. D., Sommers, C. D., Huang, H. C., Jacobsen, E. J., Tenbrink, R. E., Tomasselli, A. G., and Benson, T. E. (2010) Structural and thermodynamic characterization of the TYK2 and JAK3 kinase domains in complex with CP-690550 and CMP-6. *J. Mol. Biol.* **400,** 413–433
28. Liang, J., Tsui, V., Van Abbema, A., Bao, L., Barrett, K., Beresini, M., Berezhkovskiy, L., Blair, W. S., Chang, C., Driscoll, J., Eigenbrot, C., Ghilardi, N., Gibbons, P., Halladay, J., Johnson, A., Kohli, P. B., Lai, Y., Liimatta, M., Mantik, P., Menghrajani, K., Murray, J., Sambrone, A., Xiao, Y., Shia, S., Shin, Y., Smith, J., Sohn, S., Stanley, M., Ultsch, M., Zhang, B., Wu, L. C., and Magnuson, S. (2013) Lead identification of novel and selective TYK2 inhibitors. *Eur. J. Med. Chem.* **67,** 175–187
29. Fry, D. W., Bridges, A. J., Denny, W. A., Doherty, A., Greis, K. D., Hicks, J. L., Hook, K. E., Keller, P. R., Leopold, W. R., Loo, J. A., McNamara, D. J., Nelson, J. M., Sherwood, V., Smaill, J. B., Trumpp-Kallmeyer, S., and Dobrusin, E. M. (1998) Specific, irreversible inactivation of the epidermal growth factor receptor and erbB2, by a new class of tyrosine kinase inhibitor. *Proc. Natl. Acad. Sci. U.S.A.* **95,** 12022–12027
30. Hur, W., Velentza, A., Kim, S., Flatauer, L., Jiang, X., Valente, D., Mason, D. E., Suzuki, M., Larson, B., Zhang, J., Zagorska, A., Didonato, M., Nagle, A., Warmuth, M., Balk, S. P., Peters, E. C., and Gray, N. S. (2008) Clinical stage EGFR inhibitors irreversibly alkylate Bmx kinase. *Bioorg. Med. Chem. Lett.* **18,** 5916–5919
31. Liu, Q., Sabnis, Y., Zhao, Z., Zhang, T., Buhrlage, S. J., Jones, L. H., and Gray, N. S. (2013) Developing irreversible inhibitors of the protein kinase cysteinome. *Chem. Biol.* **20,** 146–159
32. Eastwood, B. J., Farmen, M. W., Iversen, P. W., Craft, T. J., Smallwood, J. K., Garbison, K. E., Delapp, N. W., and Smith, G. F. (2006) The minimum significant ratio: a statistical parameter to characterize the reproducibility of potency estimates from concentration-response assays and estimation by replicate-experiment studies. *J. Biomol. Screen.* **11,** 253–261
33. Goedken, E. R., Devanarayan, V., Harris, C. M., Dowding, L. A., Jakway, J. P., Voss, J. W., Wishart, N., Jordan, D. C., and Talanian, R. V. (2012) Minimum significant ratio of selectivity ratios (MSRSR) and confidence in ratio of selectivity ratios (CRSR): quantitative measures for selectivity ratios obtained by screening assays. *J. Biomol. Screen.* **17,** 857–867
34. Otwinowski, Z., and Minor, W. (1997) Processing of x-ray diffraction data collected in oscillation mode. *Methods Enzymol.* **276,** 307–326
35. McCoy, A. J., Grosse-Kunstleve, R. W., Storoni, L. C., and Read, R. J. (2005) Likelihood-enhanced fast translation functions. *Acta Crystallogr. D Biol. Crystallogr.* **61,** 458–464
36. Storoni, L. C., McCoy, A. J., and Read, R. J. (2004) Likelihood-enhanced fast rotation functions. *Acta Crystallogr. D Biol. Crystallogr.* **60,** 432–438
37. Read, R. J. (2001) Pushing the boundaries of molecular replacement with maximum likelihood. *Acta Crystallogr. D Biol. Crystallogr.* **57,** 1373–1382
38. Jones, T. A., Zou, J. Y., Cowan, S. W., and Kjeldgaard, M. (1991) Improved methods for building protein models in electron density maps and the location of errors in these models. *Acta Crystallogr. A* **47,** 110–119
39. Bricogne, G., Blanc E., Brandl, M., Flensburg, C., Keller, P., Paciorek, W., Roversi, P., Sharff, A., Smart, O. S., Vonrhein, C., Womack, T. O. (2011) BUSTER version 2.9.7, Global Phasing Ltd., Cambridge, UK
40. Emsley, P., Lohkamp, B., Scott, W. G., and Cowtan, K. (2010) Features and development of Coot. *Acta Crystallogr. D Biol. Crystallogr.* **66,** 486–501
41. Zhu, K., Borrelli, K. W., Greenwood, J. R., Day, T., Abel, R., Farid, R. S., Harder, E. (2014) Docking covalent inhibitors: a parameter free approach to pose prediction and scoring. *J. Chem. Inf. Model.* **54,** 1932–1940
42. Gehringer, M., Pfaffenrot, E., Bauer, S., and Laufer, S. A. (2014) Design and synthesis of tricyclic JAK3 inhibitors with picomolar affinities as novel molecular probes. *ChemMedChem* **9,** 277–281
43. Kulagowski, J. J., Blair, W., Bull, R. J., Chang, C., Deshmukh, G., Dyke, H. J., Eigenbrot, C., Ghilardi, N., Gibbons, P., Harrison, T. K., Hewitt, P. R., Liimatta, M., Hurley, C. A., Johnson, A., Johnson, T., Kenny, J. R., Bir Kohli, P., Maxey, R. J., Mendonca, R., Mortara, K., Murray, J., Narukulla, R., Shia, S., Steffek, M., Ubhayakar, S., Ultsch, M., van Abbema, A., Ward, S. I., Waszkowycz, B., and Zak, M. (2012) Identification of imidazo-pyrrolopyridines as novel and potent JAK1 inhibitors. *J. Med. Chem.* **55,** 5901–5921
44. Van Epps, S., Fiamengo, B., Edmunds, J., Ericsson, A., Frank, K., Friedman, M., George, D., George, J., Goedken, E., Kotecki, B., Martinez, G., Merta, P., Morytko, M., Shekhar, S., Skinner, B., Stewart, K., Voss, J., Wallace, G., Wang, L., Wang, L., and Wishart, N. (2013) Design and synthesis of tricyclic cores for kinase inhibition. *Bioorg. Med. Chem. Lett.* **23,** 693–698
45. Styles, M. L., Zeng, J., Treutlein, H. R., Wilks, A. F., Kling, M. R., Bu, X., and Burns, C. J. (July 21, 2005) Preparation of benzimidazolylazines and related compounds as selective JAK3 kinase inhibitors. International Patent WO 2005066156 A1
46. Shuai, K., and Liu, B. (2003) Regulation of JAK-STAT signalling in the immune system. *Nat. Rev. Immunol.* **3,** 900–911
47. Verma, A., Kambhampati, S., Parmar, S., and Platanias, L. C. (2003) Jak family of kinases in cancer. *Cancer Metastasis Rev.* **22,** 423–434
48. Sonbol, M. B., Firwana, B., Zarzour, A., Morad, M., Rana, V., and Tiu, R. V. (2013) Comprehensive review of JAK inhibitors in myeloproliferative neoplasms. *Ther. Adv. Hematol.* **4,** 15–35
49. Kawamura, M., McVicar, D. W., Johnston, J. A., Blake, T. B., Chen, Y. Q., Lal, B. K., Lloyd, A. R., Kelvin, D. J., Staples, J. E., and Ortaldo, J. R. (1994) Molecular cloning of L-JAK, a Janus family protein-tyrosine kinase expressed in natural killer cells and activated leukocytes. *Proc. Natl. Acad. Sci. U.S.A.* **91,** 6374–6378
50. Ihle, J. N., and Gilliland, D. G. (2007) Jak2: normal function and role in hematopoietic disorders. *Curr. Opin. Genet. Dev.* **17,** 8–14
51. Feng, J., Witthuhn, B. A., Matsuda, T., Kohlhuber, F., Kerr, I. M., and Ihle, J. N. (1997) Activation of Jak2 catalytic activity requires phosphorylation of Y1007 in the kinase activation loop. *Mol. Cell Biol.* **17,** 2497–2501
52. Quelle, F. W., Wang, D., Nosaka, T., Thierfelder, W. E., Stravopodis, D., Weinstein, Y., and Ihle, J. N. (1996) Erythropoietin induces activation of Stat5 through association with specific tyrosines on the receptor that are not required for a mitogenic response. *Mol. Cell Biol.* **16,** 1622–1631
53. Fleischmann, R., Cutolo, M., Genovese, M. C., Lee, E. B., Kanik, K. S., Sadis, S., Connell, C. A., Gruben, D., Krishnaswami, S., Wallenstein, G., Wilkinson, B. E., and Zwillich, S. H. (2012) Phase 2B dose-ranging study of the oral JAK inhibitor tofacitinib (CP-690,550) or adalimumab monotherapy *versus* placebo in patients with active rheumatoid arthritis with an inadequate response to DMARDs. *Arthritis Rheum.* **64,** 617–629
54. Kremer, J. M., Cohen, S., Wilkinson, B. E., Connell, C. A., French, J. L., Gomez-Reino, J., Gruben, D., Kanik, K. S., Krishnaswami, S., Pascual-Ramos, V., Wallenstein, G., and Zwillich, S. H. (2012) A Phase 2B dose-ranging study of the oral JAK inhibitor tofacitinib (CP-690,550) *versus* placebo in combination with background methotrexate in patients with active rheumatoid arthritis and inadequate response to methotrexate alone. *Arthritis Rheum.* **64,** 970–981
55. Denny, W. A. (2002) Irreversible inhibitors of the erbB family of protein tyrosine kinases. *Pharmacol. Ther.* **93,** 253–261
56. Evans, E. K., Tester, R., Aslanian, S., Karp, R., Sheets, M., Labenski, M. T., Witowski, S. R., Lounsbury, H., Chaturvedi, P., Mazdiyasni, H., Zhu, Z., Nacht, M., Freed, M. I., Petter, R. C., Dubrovskiy, A., Singh, J., and Westlin, W. F. (2013) Inhibition of Btk with CC-292 provides early pharmacodynamic assessment of activity in mice and humans. *J. Pharmacol. Exp. Ther.* **346,** 219–228
57. Honigberg, L. A., Smith, A. M., Sirisawad, M., Verner, E., Loury, D., Chang, B., Li, S., Pan, Z., Thamm, D. H., Miller, R. A., and Buggy, J. J. (2010) The Bruton tyrosine kinase inhibitor PCI-32765 blocks B-cell activation and is efficacious in models of autoimmune disease and B-cell malignancy. *Proc. Natl. Acad. Sci. U.S.A.* **107,** 13075–13080
58. Rankin, A. L., Seth, N., Keegan, S., Andreyeva, T., Cook, T. A., Edmonds, J., Mathialagan, N., Benson, M. J., Syed, J., Zhan, Y., Benoit, S. E., Miyashiro, J. S., Wood, N., Mohan, S., Peeva, E., Ramaiah, S. K., Messing, D., Homer, B. L., Dunussi-Joannopoulos, K., Nickerson-Nutter, C. L., Schnute, M. E., and Douhan, J., 3rd (2013) Selective inhibition of BTK prevents murine lupus and antibody-mediated glomerulonephritis. *J. Immunol.* **191,** 4540–4550
59. Solca, F., Dahl, G., Zoephel, A., Bader, G., Sanderson, M., Klein, C., Kraemer, O., Himmelsbach, F., Haaksma, E., and Adolf, G. R. (2012)

Target binding properties and cellular activity of afatinib (BIBW 2992), an irreversible ErbB family blocker. *J. Pharmacol. Exp. Ther.* **343,** 342–350

60. Singh, J., Petter, R. C., and Kluge, A. F. (2010) Targeted covalent drugs of the kinase family. *Curr. Opin. Chem. Biol.* **14,** 475–480
61. Liu, K. D., Gaffen, S. L., Goldsmith, M. A., and Greene, W. C. (1997) Janus kinases in interleukin-2-mediated signaling: JAK1 and JAK3 are differentially regulated by tyrosine phosphorylation. *Curr. Biol.* **7,** 817–826
62. Haan, C., Rolvering, C., Raulf, F., Kapp, M., Drückes, P., Thoma, G., Behrmann, I., and Zerwes, H. G. (2011) Jak1 has a dominant role over Jak3 in signal transduction through γc-containing cytokine receptors. *Chem. Biol.* **18,** 314–323
63. Potashman, M. H., and Duggan, M. E. (2009) Covalent modifiers: an orthogonal approach to drug design. *J. Med. Chem.* **52,** 1231–1246
64. Zhang, J., Yang, P. L., and Gray, N. S. (2009) Targeting cancer with small molecule kinase inhibitors. *Nat. Rev. Cancer* **9,** 28–39